Optimization of Electrospinning Parameters to Fabricate Aligned Nanofibers for Neural Tissue Engineering

A THESIS SUBMITTED IN PARTIAL FULFILLMENT

OF THE REQUIREMENT FOR THE DEGREE OF

Master of Technology

In

Biotechnology & Medical Engineering

By

MONIKA RAJPUT

210BM2014

Under the Supervision of

Dr (Prof.) B.P NAYAK

Department Of Biotechnology And Medical Engineering

National Institute Of Technology Rourkela

2012

Dr (Prof). B.P Nayak

Assistant Professor

Department of Biotechnology & Medical Engineering

National Institute of Technology, Rourkela, Orissa, India

Certificate

This is to certify that the thesis entitled **"Optimization of Electrospinning Parameters to Fabricate Aligned Nanofibers for Neural Tissue Engineering"** by **Monika Rajput (210bm2014),** submitted to the National Institute of Technology, Rourkela for the Degree of Master of Technology is a record of bonafide research work, carried out by her in the Department of Biotechnology and Medical Engineering under my supervision and guidance. To the best of my knowledge, the matter embodied in the thesis has not been submitted to any other University/ Institute for the award of any Degree or Diploma.

Dr (Prof). B.P Nayak

Assistant Professor

Department of Biotechnology and Medical Engineering

NIT Rourkela

ACKNOWLEDGEMENT

Apart from the efforts of me, the success of my project depends largely on the encouragement and guidelines of many others. I take this opportunity to express my thankfulness and appreciation to those individuals who have been involved in the successful completion of this project.

First and foremost I would like to express my deep sense of gratitude and respect towards my guide **Dr. (Prof) B.P Nayak**, Department of Biotechnology and Medical Engineering, NIT Rourkela for his tremendous support and constant guidance throughout my project. I also thank him for encouraging me to do something new.

I extend my sincere thanks to **Prof G.S Hotta**, Department of Chemistry, NIT Rourkela for allowing me to use the lab facilities and for pieces of advice in times. My special thanks to research scholar **Ms. Abhipsa Mahapatra**, without her help this work could not be completed. I would like to thank **Mr. Ashwini Kumar**, who helped me to solve many problems of my work.

Words are inadequate in offering thanks to my friends **Daisy Soni, Smita Priyadarshini Pilla, Maneesha Pandey, Divyanshu Mahajan, Harsh Vardhan Sharma** and all others for their encouragement and strong support in carrying out this project.

Finally, yet importantly, I would like to express my heartfelt thanks to my parents **Mr. Kalicharan** and **Mrs. Krishna** and my brother **Mayank** and all my family members, for their blessings, support, and for constant encouragement during my good and bad times and very special thanks to **God** for showering the best blessings on me.

Monika Rajput

TABLE OF CONTENT

LIST OF FIGURES

LIST OF TABLES

Abstract

Electrospinning is the most promising method to fabricate random as well as aligned fibers in nanoscale. The scaffolds with embedded nanofibers have successfully been used for *in vitro* proliferation and differentiation of stem cells into various lineages for specific tissue engineering. Currently, a lot of effort is being put to optimize electrospinning set up for producing aligned nanofibers since scaffolds with aligned nanofibers can be propagative to neuronal cells for engineering neurons. In case of neuronal damage, aligned nanofibers have the potential to guide the axonal regeneration and neurite extension in a polarized manner on the parent nerve fiber leading to regeneration. The main objective of current study is to electrospun the aligned nanofibrous scaffolds from poly-ε-caprolactone (PCL) for its potential application in neural tissue engineering. Briefly, for electrospinning of PCL solution, the correct solvent system, their ratios and other process parameters were optimized. A solvent system of chloroform and methanol was used with an initial ratio of 3:1respectively. The electrospinning trials were conducted with a fixed plate distance of 10cm, the flow rates range of 1-2ml/hr (0.5 ml increment), and an applied voltage of 10- 14 KV (2 kV increment) for 30 second in each run. Determining the best process parameters, the polymer solution tested at 6-12% (w/w) of PCL (2% increment). Within each concentration three different solvent systems (chloroform: methanol, dichloro methane: dimethyl formamide, chloroform + dichloro methane: dimethyl formamide and chloroform: dimethyl formamide) and within each solvent mix five different solvent ratios (1:1 to 5:1) were tested. Post electrospinning characterization by optical and scanning electron microscopes (SEM) concluded the best optimized parameters as: a solvent system of chloroform + dichloromethane: methanol (3:1 ratio) , 10% (w/w) PCL, 10cm of spinning distance, a flow rate of 1ml/hr and an applied voltage of 12 KV. With these parameters,

fibers produced were uniform, continuous and the average diameter was in a range of 350to 480nm. The best set of parameters was used for electrospinning aligned nanofibers with an array of in house designed collectors i.e. air gap metallic strip collector, parallel magnetic collector, frame collector and copper grid collector. The optical microscopy and SEM analysis showed that the copper grid collector produced best aligned nanofibers that were further confirmed by Fast Fourier Transformation (FFT) of image. The range of fiber diameter produced was 330 to 560 nm. The current study established the best electrospinning parameters for PCL and the best collector set up to produce aligned nanofibers for neural tissue engineering applications.

Keywords: Neural Tissue Engineering; Scaffold; Poly (ε-caprolactone); Electrospinning; Solution Parameters; Process Parameters; Collectors Design; Aligned Uniform Continuous Nanofibers;

CHAPTER ONE

INTRODUCTION

1. Introduction

Human nervous system is a box of information and it is important to understand the complex relationship with the components of central and peripheral nervous system. This information plays vital role in deciphering the causes of neural disorders and provides an effective therapy for the treatment of ischemic, congenital, or neurodegenerative disorders (1). The treatment of neural damages requires an extra care because axons do not regenerate easily in their native environment. So, it is necessary to provide permissive environment for nerve regeneration (2).

Currently, there are two approaches for the treatment of neural damages, either direct end to end surgical connection of the injured nerves, this approach repairs only small defects or gaps in the nerve. For large nerve defects this approach is not suitable because load during reconnection of nerves may inhibit regeneration of nerves. So, to treat the large nerve gaps defects, the other approach autologous nerve grafting have been used. Autografts avoid an immune response in the patient on implantation, but there are certain limitations in this approach such as donor site morbidity and limited availability (3). So, an alternative approach is to develop nerve guidance conduit (NGC) that would provide path for nerve out-growth and promote regeneration of nerves and it is possible only by utilizing the principle of tissue engineering. Tissue engineering is the breakthrough advancement in the field of "Biomedical Engineering".

1.1 Tissue Engineering

Tissue engineering has emerged as an excellent approach in the human health care, which applies principles of engineering and the life sciences together to develop a biological substitute to restore maintain or improve the function of damaged tissues and organs. Tissue engineering has broad range of application in regenerative medicine and provides most suitable way to repair damages (4). Tissue engineering research mainly focuses in regulation of cell behavior and tissue

organization in damaged area through the development of synthetic extracellular matrices (ECM) also known as scaffold, which provide support to the three-dimensional cell culture and tissue regeneration (4, 5). The main goal of this technology is to create new bio-artificial tissues by the combination of three components known as triad: scaffold (support system), cells and growth factors (5).

1.1.1 Neural Tissue Engineering

Neural tissue engineering is the sub-specific field of tissue engineering. Tissue engineering in the nervous system is the technology of designing and creating suitable support where neural tissues/ cells organized themselves in a controlled manner for therapeutic purpose in the nervous system. Neural tissue engineering (NTE) is a rapidly growing research area which is providing new approach to repair and regenerate damaged nerves by creating suitable environment (6). So, it is important to design and develop the novel scaffolds which are able to guide neurite growth for axonal regeneration through damaged areas of central and peripheral nervous system. The desired properties of scaffold for nerve regeneration are biocompatible, mimic native extra cellular matrix environment with appropriate mechanical strength as in human system, non immunogenic, biodegradable with non toxic products, degradation rate of scaffold should match up with the growth of axons through the injured site (6).

There are several fabrication techniques which have been used to develop nanofibrous scaffolds to achieve the goal of neural tissue engineering such as self assembly and phase separation with various drawbacks like time consuming effort, uncontrolled fiber diameter and alignment. Whereas, a spinning technique called “electrospinning” circumvent all drawbacks of these previous methods. Using electrospinning techniques, nanofibers can be formed into random / aligned a mesh which provides the pathway for nerve regeneration.

1.2 Electrospinning

Aligned nanofibers are particularly required for nerve regeneration as these fibers guide the neurite outgrowth in a particular direction along the natural axis and electrospinning enables the fabrication of these nanofibers. These nanofibers have fiber diameters much smaller than those produced form other conventional technique and enhance cell proliferation and attachment to the surface of scaffold in order to penetrate inside the 3-D structure of scaffold.

The mechanism behind the Electrospinning technique is utilization of high electrostatic potential to produce fibers scaffold. It consists of four parts: syringe pump to control flow rate, syringe with needle which act as one of the electrode to charge the polymer solution, power supply to generate electric field, and collector which act as other grounded electrode to collect fibers. Under the influence of electric field, charge developed in the polymer solution. At low electric field strength, a pendant drop emerged out from the tip of needle which is balanced by the surface tension of solution. As the voltage increased, charges on solution repel each other which results in elongation of drop into conical shape known as taylor cone due to electrostatic forces in opposite direction to surface tension. As the voltage reached to its critical value, all equilibrium forces on drop get distorted and the electrostatic forces overcomes the surface tension due to which, a jet is emerged out of the cone and get deposited on grounded electrode as shown in figure 1.1.

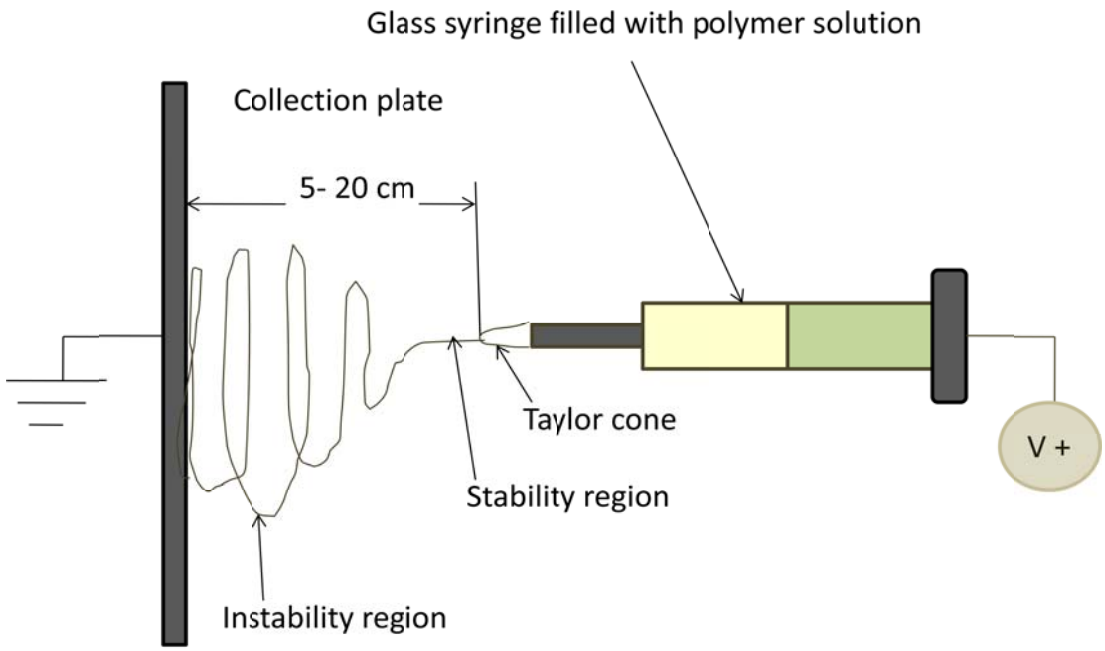

Figure 1.1 Schematic Diagram of Typical Electrospinning Setup

Some researchers explained the parameters that govern the whole electrospinning process such as: solution parameters (polymer concentration, solvent system and conductivity etc.), process parameters (flow rate, applied voltage, distance between needle tip and grounded collector and collector design), and the ambient parameters (temperature and relative humidity). These parameters control the uniformity, continuity and nano range of fiber diameter and fabrication of aligned nanofibers (7). Specifically, the objective behind the research is to optimize the electrospinning parameters to obtain aligned nanofibrous Poly caprolactone (PCL) scaffold to improve and compare the growth of cells and differentiation on aligned and random PCL scaffolds. It is hypothesized that PCL nanofibrous scaffold and their easy manipulation characteristics will be able to enhanced the neurite growth and provide the appropriate support and structure that have the potential for successful transplantation in the future.

CHAPTER TWO

LITERATURE SURVEY

2. Review of literature

2.1 Importance of Tissue Engineering

The area of tissue engineering came into existence in response to the problems such as organ damages and their repairing. Tissue engineering is a new approach which solved the mystery of repairing and replacement of the damaged tissues or organs (8). In 1993 Langer and Vacanti defined tissue engineering, as an interdisciplinary field that include the principles of engineering and life sciences for the creation of biological substitute to restore, repair or replace the damaged tissue or their functions and understand the interactive properties of cells with the support system (9). According to the national science foundation, it is the most simple and convenient technique to create living tissues for therapeutic purposes. There are many other similar definitions in literature which involved extracellular matrices, implants and biodegradable/ non-biodegradable scaffolds of biomaterials. Some of these definitions are:

- It is the process of developing living, three dimensional cells or tissues by utilizing the specific components- cells, support system that is scaffold and growth signals (10)
- It is the combination cells scaffold material, and bioactive proteins which are used to repair or developing of new cells or tissues (11).
- It is the field of biomedical engineering which exploits the living cells such as stem cells in various ways to repair, restore and maintain the function of cells or tissues (12).
- It is the process that combines (a) living cells with biomaterials, (b) utilization of stem cells as therapeutic tool and, (c) create tissues in-vitro for implantation (13).

Tissue engineering relies on the basic three components known as triad system to achieve the restoring and repairing of damaged tissue or its function (5): (1) Construction of support system commonly known as scaffold with desired properties from biomaterials of desired properties, provides three dimensional structure matrices where cells can be grown from the host tissues in-

vitro or in-vivo (14, 15), (2) Use of cells either adult or embryonic stem cells or tissue specific adult cells of any of the stage, differentiation or maturation, can be seeded on the scaffold and implanted in the body to restore the damaged functions of organs or tissues (16), (3) chemical signal in form of growth factors such as neurotrophic factors for nerve cells, fibroblast growth factors which help the stem cells to grow in respective cell lineages (17).

Many researchers working on bone tissue engineering in order to develop damaged bone substitute or implant (18), cartilage tissue engineering (19), nerve tissue engineering (20, 21) and skin tissue engineering (22). Skin tissue engineering graft such as Apligraft and Dermagraft has been already available as a therapeutic medication (22, 23).

This thesis mainly focus on neural tissue engineering because the behavior of nerve regeneration is very unique, as nervous system consist of soft tissues, so needed support system in the form of nanofibers which have been found to be the best scaffolding that guide the outgrowth in a particular direction in a directed manner as in the human system.

2.1.1 Role of Neural Tissue Engineering

The nervous system presents a greater challenge in front of the field of tissue engineering because the chemical and anatomical structure of nervous system is just start to be understood. Due to advancements in material science engineering in combination with molecular neurobiology and gene transfer techniques made it possible for tissue engineering to solve the problems related to nervous system (24). Therefore, neural tissue engineering involves in finding the issues those concern with selection and use of cellular components, and the mode of organization that is intracellular interaction or the interaction between cells and environment of cellular components (25, 26). Currently, tissue engineering deals with the therapeutic measurements in the nervous system:

- The replacement of absent neuro-active components functionally.

- To repair or regenerate the degenerated or damaged neural tissues.
- The developing of neural cell based biosensor and neural circuits.

The nervous system has the unique ability to regenerate the damaged nerves by its own. The most severe injury in nervous system is the complete transection of the nerve fiber. The protease activity comes into action after injury and initiating a series of events of degradation at the distal ends of the injury. Where the new axons again regenerated from the unmyelineated region of the nodes of Raniver, but it was reported that the rate of axon regeneration in humans to be 2 mm / day (27). To repair large nerve defects, it takes over the month. At that time the golden approach to treat the damages is autologous grafting but the disadvantage is donor site morbidity. So, neural tissue engineering may be the right approach to bridge those defects.

The potential of neural cells to regenerate have been investigated by many researchers. Girard et al. observed that the use of autologous Schwann cells enhances the regeneration of neurons and remyelinization as it secrets adhesion molecules (N-CAM), nerve growth factors (NGF), brain derived neurotrophic factor (BDNF) but also shown the inhibition effects on migration of cells to CNS and it delayed the repairing process (28).

In 2004, Recknor et al. investigated role of astrocytes in neurogenesis from the adult neural stem cells and found that the growth of astrocytes is in directed manner which was a novel approach to provide controlled growth and differentiation of neural stem cells (29). But due to the secretion of certain signal astrocytes have the cytotrophic effect which inhibits the regeneration of nerves. Many researchers tried to improve these cytotrophic effects during regeneration (30).

In 2009, David et al. implanted PLLA scaffold plated with olfactory ensheathing cells (OEC) in the brain and found that olfactory system provides the axonal regeneration into both central

nervous system as well as peripheral nervous system. He also stated that the OEC phenotype is closer to that of Schwann cells and have properties of both Astrocytes and Schwann cells (31).

In neural tissue engineering, the engineered scaffold seeded with the specific type of cell which repair or restore the lost function. As the nerve regeneration requires an extra care for that scaffold should well design mimics the extracellular matrix and provide correct signals for cell growth, proliferation, differentiation and eventually formation of tissue (32).

Neural tissues are soft tissues so for their growth, therefore, the support system should be in fiber mesh form. Recently many researchers designed the materials which can guide the neural tissues to grow. In 2003, Handlock et al. developed aligned conduit consist of stack membranes of polymer over the poly teflon tube and seeded with Schwann cells and showed that the regeneration of nerves along the natural axis directed in a particular direction without crossing as compared to random scaffold (33). Similar results with aligned conduit reported by the Stokols and Tuszynski in 2006 (34).

In 2007 Corey et al. designed a substrate created by electrospinning of Poly-L lactic acid nanofiber over the layer of Poly-o-glycolic acid which attach fiber to the glass and not toxic to the primary neurons. After plating of motor neuron in serum free conditions on engineered scaffold found that the alignment of neurons grown on scaffold was same as the alignment of nanofibers in scaffold (35, 36). He also stated that electrospun aligned nanofibers are the most suitable support for the nerve regeneration.

2.1.1.1 Biomaterials for Nerve Regeneration

There are various natural and synthetic polymers which have been investigated for fabricating scaffolds for repairing damage of the nervous system. The material to be used to fabricate

scaffold should be biocompatible, biodegradable, no immunologic response and with good surface and mechanical properties (5).

Natural polymers such as collagen, silk fibroin, gelatin, and alginate have studied for neural tissue engineering. Out of them collagen has been studied extensively. In 2009 Alluin et al. used collagen to construct nerve conduit and implanted in the brain to repair the peripheral nerve injury and he observed that nerves grow in a directed manner on conduits and fill the nerve defects (37). After many researches collagen has been approved by Food Administrative Department (FDA) for its use in humans. FDA approved nerve guide Neuragen recently showed the formation on neuroma in 2 cm gap human median. So the existing nerve conduits are not appropriate to be used in nerve regeneration for large gaps (38).

In 2010, Madduri et al. developed silk fibroin nerve conduits with modification which promise to enhance the recovery of damaged peripheral nerves functions. They used the silk fibroin membranes loaded with neurotrophic factors (NGF and GDNF) as a base on which nanofibers deposited randomly and in aligned way through electrospinning method. They used parallel electrode system to produce aligned fiber and flat plate for random fibers. Dorsal root ganglia (DRG) sensory neurons and spinal cord (SpC) motor neurons seeded on both scaffolds and he observed that both sensory and motor neurons from chicken embryo, grow along the axis of aligned fiber and rate of outgrowth is faster as compared to random scaffold. They also analyzed the growth of nerve tissue by using S-100 cell marker for glial cells (39).

But the natural polymers lack in mechanical strength so researchers focused in using synthetic biodegradable polymers such as PLGA, PLLA, poly caprolactone (PCL) and conducting polymers: polypyrrole, polyaniline for neural applications. In 2005, Yang et al. employed the use of PLLA to fabricate nanofibrous scaffold for nerve injury repair. He seeded the DRG sensory

neurons on scaffold and showed that the scaffold support the extension of neurons (40). Similar work has shown by many researchers using PLGA, Hydrogel and PCL (41, 42, and 43).

In 2007, Gomez and Schimdt used conducting polymer polypyrrole for enhancing the neurite extension. They immobilized nerve growth factors with the help of arylazido functional group conjugated with polyallylamine on the surface of electrically conducting polymer polypyrrole and conducted electrical simulation experiments and revealed that there was 50 % increase in neurite extension as compared without electrical simulation one. They stated that there was slight decrease in conductivity as compared to other modification approaches (44).

Synthetic polymers lacking biological functional groups for cell adhesion, so they are modifies by various methods like plasma treatment (42). The other approach is composite scaffold of natural and synthetic polymer which overcomes each others limitation. As natural polymers are hydrophobic and having functional groups for cell adhesion and synthetic polymers having good mechanical strength. These composite scaffolds have all desired properties required for neural scaffold. In 2008, Ramakrishna et al. fabricated PCL and gelatin composite of various ratios. They cultured nerve stem cells (C17.2) on composite scaffold and found that the PCL / Gelatin scaffold of 70: 30 ratio enhanced the proliferation and differentiation of nerve stem cells as compared to PCL and Gelatin scaffold (43). Likewise many scaffolds have been prepared and tested for neural applications: PCL/ collagen (45), PCL and Polysaccharide (46), Alginate/ chitosan (47). So these biomaterials have been selected on the basis of which damaged area to be repaired.

2.2 Different Fabrication Methods of Scaffolds

Scaffolds are the basic component of tissue engineering. The desired properties of neural scaffold that it should be biodegradable and its degradability rate should match up with the

formation of tissues at the damaged area, biocompatible, having good biomechanical properties such as pore size and porosity, and the most important is that it should mimic the exact orientation or structure as of extracellular matrix and its environment. For the growth of neural tissue, the scaffold should be in nanofibers form or aligned so that it guides the axonal extension through the injured environment (5, 7).

Several fabrication methods have been developed to fabricate three dimensional (3-D) scaffolds for neural tissue engineering implants. The conventional techniques used for scaffolds fabrication including self assembly, phase separation, template method, 3-D printing, melt spinning and electrospinning.

The self assembly method utilizes the pre-existing components to organize themselves into desired patterns and functions. This method is time consuming sometimes it takes day to fabricate the nanofibrous scaffold and not able to produce fibers in bulk. The phase separation method is a multi-process including dissolution, extraction using different solvents, freezing, and gelation. All these methods results in a micro to nanoscale fibrous scaffold. Where this method also time taking and not produce regular nanofibers.

The template method uses a already prepared nanofibrous membrane as a template to produce nanofibers of solid or hollow shape. This method fabricates nanometer range tubules and fibrils of various materials. But the limitation of this method is that it cannot produce single continuous fiber. Nanofibers are also prepared by using multi component fiber technique consist of desired and soluble polymer. The soluble polymer is dissolved out from the composite and remaining is microfilament. But the yield of this process is very low. Where Pike et al. (7) modified this process of fabricating nanofibers by splitting of fibers in melt spinning process. He produced fibers with low diameter of 200 nm range.

Therefore, electrospinning process is the only promising approach for the production of uniform and continuous nanofibers from various biomaterials in mass. And as per the requirement of neural tissue engineering, scaffold is made up of aligned nanofibers, though random mesh of nanofibers also support the growth of neural cells but the density, proliferation and differentiation is very low as compared to aligned nanofibrous scaffold. Developing aligned nanofibrous scaffold is seems to be feasible by the only method known as “Electrospinning”.

2.3 Electrospinning of Nanofibers and Its Mechanism

The most promising method for fabricating nanofibers is the electrostatic spinning or electrospinning process. The electrospinning process, which was first investigated by Rayleigh in 1897 and its detailed studies done by Zeleny in 1914 and was first patented by Formhals in 1934 (48). This method made possible to produce polymeric fibers with diameters in the range of nanometers to microns, and it all depending on the type of polymer and the processing conditions used. It includes the generation of a strong electric field between a polymer solution filled in a glass syringe with a capillary tip or metal needle, and a collection plate. When the voltage reaches a critical value, the electrostatic force overcomes the surface tension on the taylor cone which is suspended from the tip of the needle, and a jet is emerged out from the cone. The diameter of charged jet decreases under the influence of electrostatic forces and under certain operating conditions, bending stabilities inducing extensive stretching of jet before collection on the collection plate. During stretching the solvent gets evaporate and this leads to further reduction in the diameter size of emerged jet. The dried fibers get deposited randomly or in aligned way on the surface of the collection plate.

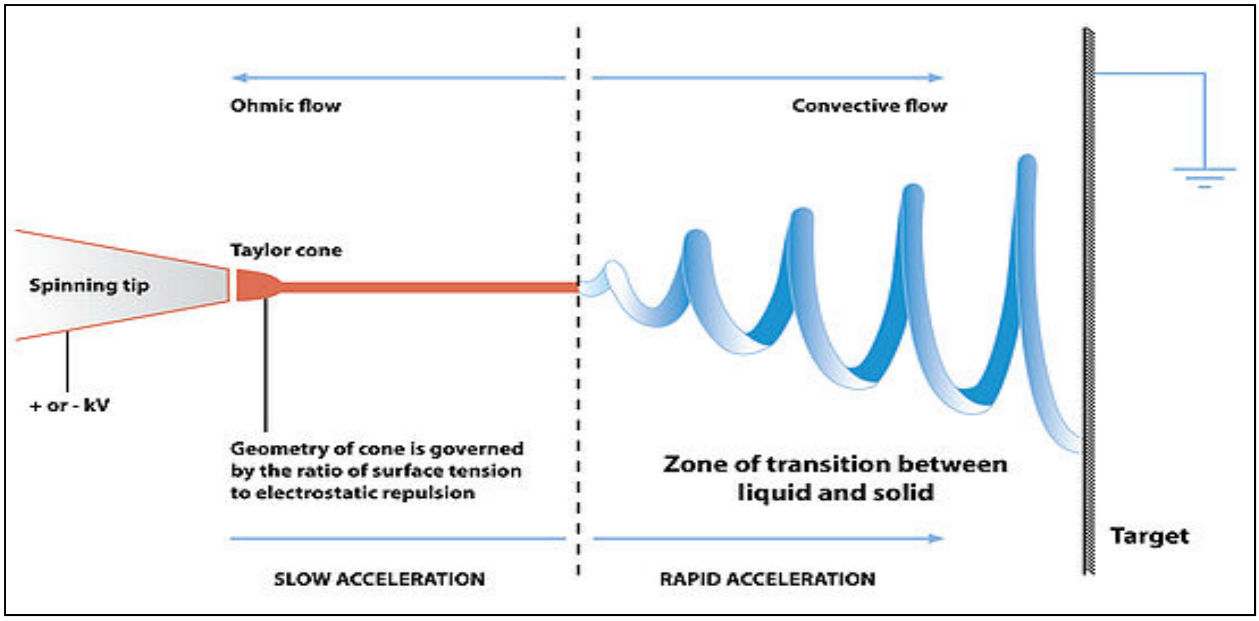

Figure 2.1 Mechanism of Electrospinning Process

The electrospinning process governed by many parameters and they are broadly classified into solution parameters, process parameters and ambient parameters. To control the diameter of fiber and alignment of fiber is an important task as concern with the neural tissue engineering. So, it is necessary to optimize the parameter which governs the electrospinning process.

2.3.1 Study of Different Parameters of Electrospinning Method

2.3.1.1 Control of Fibers Diameter

Several researches have been reported the effect of electrospinning parameters on fiber diameter and its morphology (49). These are: solution parameters- polymer concentration, viscosity, conductivity of polymer solution, type of solvent used and the process parameter- flow rate of solution, applied voltage and the distance between needle tip and the metallic collector plate.

In 1971, Baumgarten described this process with polymer solutions. He spun acrylic resin-dimethylformamide (DMF) systems at different concentrations and viscosities, and fabricate fibers, ranges from 0.05- 1.1 μm in diameter. He also stated the effects of solution viscosity and

conductivity, flow rate or other parameter on the length and diameter of the fiber. His results showed that as the viscosity of solution increased the diameter of the fiber increased. And he also mentioned that increased applied voltage increases the electrostatic forces due to which small diameter fibers are produced. He also did research on the effects of humidity on the spinning of fibers and concluded that, if the relative humidity less than 5%, droplets dried as soon as it contacts the dry air and spinning will take place for few minutes only, where if the relative humidity is more than 60 % air, the fibers produced not dry properly and deposited on collection plate without drying (50).

In 1987, Hayati *et al.* described the effect of applied voltage and environment of Taylor cone on the ability of forming stable jets. He stated that the conductivity of the polymer solution was a major parameter in determining the time of jet ejection. Under high applied voltage the conductive polymers found to drip from the needle tip and form very erratic jets that broke into many droplets. On the other hand, insulating materials were unable to hold a surface charge and therefore no electrostatic forces built up at the interface. In the case of semi-conducting fluids (conductivity in the range of 10-6 –10-8 Ω-1m-1), it was possible to form stable jets erupting from a conical base (51).

In 1993, Berry et al. also did studies on parameters which showed that the diameter of fiber created is influenced by molecular weight of polymer along with the polymer concentration. He stated that the diameter of fiber can be described on the basis of berry number index, *Be* (52).

In 1990 and 1994, Cloupeau *et al.* and Grace *et al.* studied the effects of flow rate, applied potential, capillary size, and fluid properties such as surface tension, fluid conductivity, and viscosity on the electrospinning process. Since then, this process has been used to produce various implants such as synthetic vascular grafts, tubular products, and acrylic fibers (53).

In 1995, Doshi and Reneker electrospun poly (ethylene oxide)to produce fibers with diameters ranging from 50-5000 nm. In their work, explained the electrospinning process, the processing conditions, fiber morphology, and potential applications of the fibers. In 1996, Reneker and Chun, electrospun more than 20 polymers, including polyethylene oxide, nylon, polyimide, DNA, polyaramid, and polyaniline and were able to fabricate polymer fibers with diameters ranging from 60 nm-20 μm (54).

In 2001, Ko *et al.* employed the influence of the molecular conformation of polymer in solution as predicted by *Be*, on a electrospun poly (L-lactic acid)/chloroform system and confirmed the relationship between *Be,* solution concentration and its intrinsic viscosity (55).

In 2003, Fridrikh et al. investigated the parameters that control fiber diameter on the basis of difference between the surface tension and charge repulsion due to electrostatic forces in the jet (). Many researches are still going on, to study the effect of electrospinning parameters on the electrospun fiber diameter and its morphology with different polymers (56).

2.3.1.2 Fiber Alignment and Collection Method

Recently, researchers focus on fabrication of aligned nanofibers. Alignment of nanofibers directs the neurite outgrowth and extension in a particular direction without criss crossing. Alignment of fiber affected by process parameters such as flow rate, applied voltage, distance between tip of needle and collector, and the most important parameter that influence the collection of fiber is design of collector.

There are various designs of collector which have been used by researchers to fabricate aligned nanofibrous scaffold using different polymers for neural applications such as rotator drum collector, disk collector, frame collector, patterned collector, static parallel electrode and ferrite air gap collector. In 2009, Wang et al. developed the aligned scaffold of composite of iron oxide

and poly vinyl pyrollidone of different ratios. He used parallel ferrite magnets coupled with plasma treatment (57). In 2010, John et al. developed aligned nanofibrous scaffold of poly ethylene oxide (PEO) by the introduction of magnetic field along with electric field. He used cylindrical magnet and characterization he found that aligned fiber deposited only on the top layer of magnet where at left and right face random collection (58). In 2011, Pokorny and Velebny, developed aluminum grid with sliding board mechanism to fabricate aligned nanofiber. They also found that on varying width gap between the wires or varying the angle of board with grid effect the alignment of fibers (59).

In 2005, Yang et al. described that nano-sized fiber of 300 nm of PLLA improved the differentiation of neonatal mouse cerebellum C17.2 stem cells as compared to micro-sized fibers. He also described that the elongation and orientation of neurites were along the aligned fibers direction and had the longest neurite extension on aligned nanofibers in comparison to the micro aligned and random mats of fiber. He used rotatory drum collector to fabricate aligned nanofibers (60). In 2008, Chew et al. showed that both aligned and random PCL scaffold enhanced up regulation of early myelination marker, myelin associated glycoprotein (MAG) and down regulation of immature Schwann cell marker- NCAM-1 where increased expression of myelin specific gene P0 was observed only on aligned PCL scaffold. On that basis he also stated that aligned PCL scaffold is preferred for maturation of Schwann cells (6).

In 2009, Yao et al demonstrated that nanofibers provide high proliferation rate as compared to microfibers and fiber diameter plays less role in regulating differentiation. He used PC12 neural cell lines and seeded on both aligned and nonaligned nanofibers and the results also showed that aligned PCL nanofibers had longer neurite extension in comparison to non-aligned one. He used the modification of drum collector that is disk collector (61). In 2010, Gertz et al. demonstrated

that PLLA nanofibrous scaffold enhanced the growth of sensory and motor neurons and also neurites developed earlier in comparison to the PLLA films. He did not found a significance difference in number and length of neurites on aligned or non-aligned scaffold (62). These studies suggested that aligned nanofibrous scaffold enhances proliferation, differentiation and directional neurite extension.

So the present study is to manipulate the electrospinning parameters to fabricate aligned nanofibrous scaffold of Poly caprolactone for neural tissue engineering application. Therefore, different collector designs were used to fabricate aligned fibers and their characterization was done by optical microscopy and scanning electron microscopy.

CHAPTER THREE

OBJECTIVE

3. OBJECTIVE

Recent advancement in area of tissue engineering and regenerative medicine has made possible to accomplish the most difficult task that is regenerating and restoring the whole function of lost organ or tissues, especially for nerve regeneration. And to regenerate a new organ there is requirement of support system which provide exact environment of physiological conditions for the growth of cells known as scaffold. Among many polymers, PCL was chosen due to its desired properties to fabricate neural scaffold. Electrospinning is the most convenient method to fabricate aligned nanofibrous scaffold for nerve regeneration, aligned fibers guide the nerves to extend in a directed manner along the natural axis and enhance the differentiation of cells as compared to random nanofibrous scaffold. So, aligned fibers are more favorable. Therefore, the main objective of this research work was to fabricate aligned nanofibers.

Objective of the current research work are:

1. Optimization of parameters: solution parameters – polymer concentration, solvent system and solvent ratios, process parameters: flow rate, an applied voltage and spinning distance of the electrospinning method to produce uniform, continuous and nano range fiber diameter of PCL.
2. Morphological characterization of fibers by scanning electron microscopy (SEM) for continuity, uniformity and for determination of fiber diameter.
3. Fabrication of different designs of collector: air gap metallic strip, parallel magnet and patterned copper grid collector. Using these collectors produce aligned nanofibers at optimized solution parameter and optimize the process parameter to obtain best alignment of fiber.

4. Morphological characterization of fibers by optical microscopy and SEM for fiber alignment and fiber diameter.
5. Determination of porosity of best aligned nanofibers and random nanofibers of same conditions using liquid displacement method and compare them.

CHAPTER FOUR

PLAN OF WORK

4. Plan of Work

An aligned nanofiber plays an important role in nerve tissue engineering. These nanofibers direct the growth of axons in a particular direction without diverting the pathway as compared to random nanofibers. The present project work was carried out according to the following plan to produce aligned nanofibers by using electrospinning method.

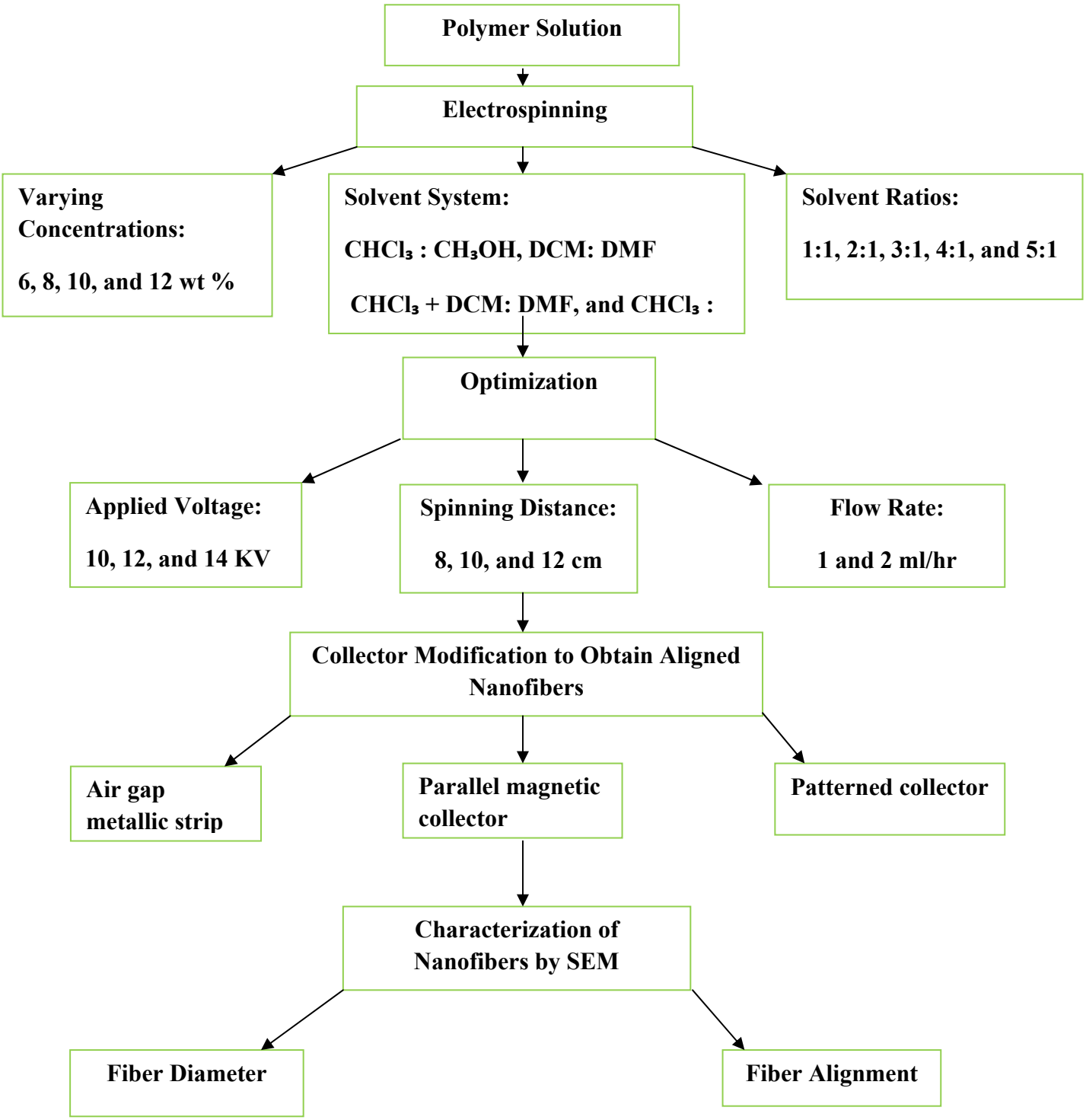

CHAPTER FIVE

MATERIALS AND METHODS

5. Materials and Methods

Poly-ε-caprolactone being used as a biomaterial in this work due to its desired neural scaffold properties such as biocompatibility, biodegradability and biomechanical strength and PCL was electrospun to obtain optimized parameters for uniform, continuous fibers and different collector set ups was used to fabricate aligned nanofibers for neural applications.

5.1 Materials

Poly (ε-caprolactone) were purchased from Sigma-Aldrich with a molecular weight Mn=80,000 in pellet form. The solvents selected to dissolve the PCL were determined from the literature review. These solvents were chloroform, dichloromethane, di-methyl formamide and methanol. The solvents were purchased from Merck Co. and used without further purification.

5.1.1 Preparation of polymer solution

All solutions for electrospinning were prepared in 5 ml quantities. Due to the solvents toxic nature, all solutions were prepared under fume hood. The polymer concentration used varied from 6 wt % to 12 wt%. Solutions were prepared by dissolving PCL in four different solvents with varying solvent ratios, ranging from 1:1 to 5:1. The different solvents and varying ratios used to prepare solution described in table. The use of solvent system was based on work by Rutledge (5). For the preparation of solution, chloroform was added first to the air tight small glass bottle and weighed polymer of 0.3 g or 0.6 g for 6wt% and 12 wt % concentration solutions respectively were added to it. In order to dissolve PCL pellets, chloroform with polymer pellets was agitated on a magnetic stirrer for first 15 minutes. After that, methanol was added to the solution while on the magnetic stirrer. The glass bottle was then sealed and the solution remained on the magnetic plate for 24 hrs at room temperature. All solutions were used for electrospinning within 5 days of the date of preparation of solution.

Table 5.1 Electrospinning Solution Parameters Varied in the Optimization Tests

Polymer Concentration	Solvent System	Solvent ratios
6 wt %	Chloroform: Methanol Di-chloromethane: Di-methylformamide Chloroform + Di-chloromethane: Di-methylformamide	1:1, 2:1, 3:1, 4:1,5:1 1:1, 2:1, 3:1, 4:1,5:1 1:1, 2:1, 3:1, 4:1,5:1
8 wt %	Chloroform: Methanol Di-chloromethane: Di-methylformamide Chloroform + Di-chloromethane: Di-methylformamide	1:1, 2:1, 3:1, 4:1,5:1 1:1, 2:1, 3:1, 4:1,5:1 1:1, 2:1, 3:1, 4:1,5:1
10 wt %	Chloroform: Methanol Di-chloromethane: Di-methylformamide Chloroform + Di-chloromethane: Di-methylformamide	1:1, 2:1, 3:1, 4:1,5:1 1:1, 2:1, 3:1, 4:1,5:1 1:1, 2:1, 3:1, 4:1,5:1
12 wt %	Chloroform: Methanol Di-chloromethane: Di-methylformamide Chloroform + Di-chloromethane: Di-methylformamide	1:1, 2:1, 3:1, 4:1,5:1 1:1, 2:1, 3:1, 4:1,5:1 1:1, 2:1, 3:1, 4:1,5:1

4.2 Scaffold Fabrication

4.2.1 Electrospinning of Solution

The electrospinning set-up which was used to produced PCL fibers as shown in figure (). The apparatus accommodated in a fume hood flushed with dry air. A high voltage DC power supply was used to supply the required charge to the solution. A high speed syringe pump was placed perpendicular to the ground. A 10 ml glass syringe were filled with PCL solution, with 22 G flat tip needle of inner diameter of 0.7 mm was used to produce fibers. The needle was connected to

the power supply positive terminal to charge the polymer solution. The iron plate which act as stage, was covered with aluminum foil and connected to the negative terminal of power supply, was used as the fiber collector. The following fixed parameters were used throughout the experiment: (a) collecting time: 1 hr, and (b) a constant room temperature of 28-37ºC and a constant relative humidity of 48-52 % was maintained by dehumidifier.

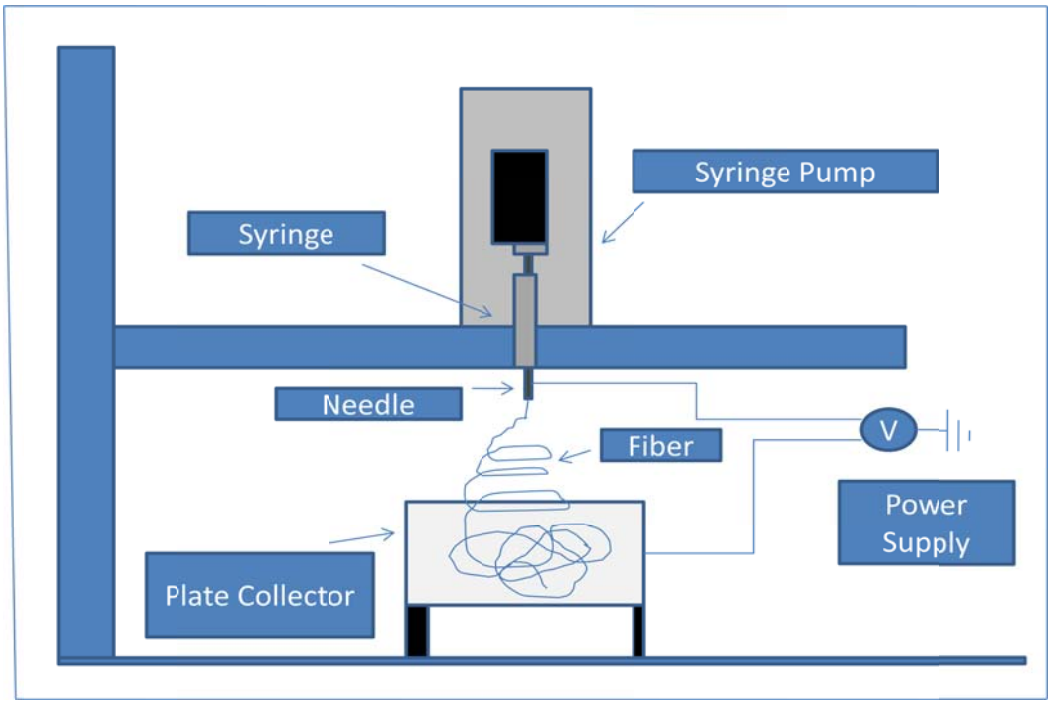

Figure 5.1 Schematic Diagram of Electrospinning Set up consist of Syringe Pump, Collector, D.C Voltage Supply.

To obtain aligned nanofibers, it was necessary to determine the optimal electrospinning process parameters: applied voltage, plate distance, flow rate and the most important parameter which is more influential on fiber alignment that is collector design. Different collector set up and other electrospinning conditions were tested to produce aligned nanofibers as shown in table 4.2.

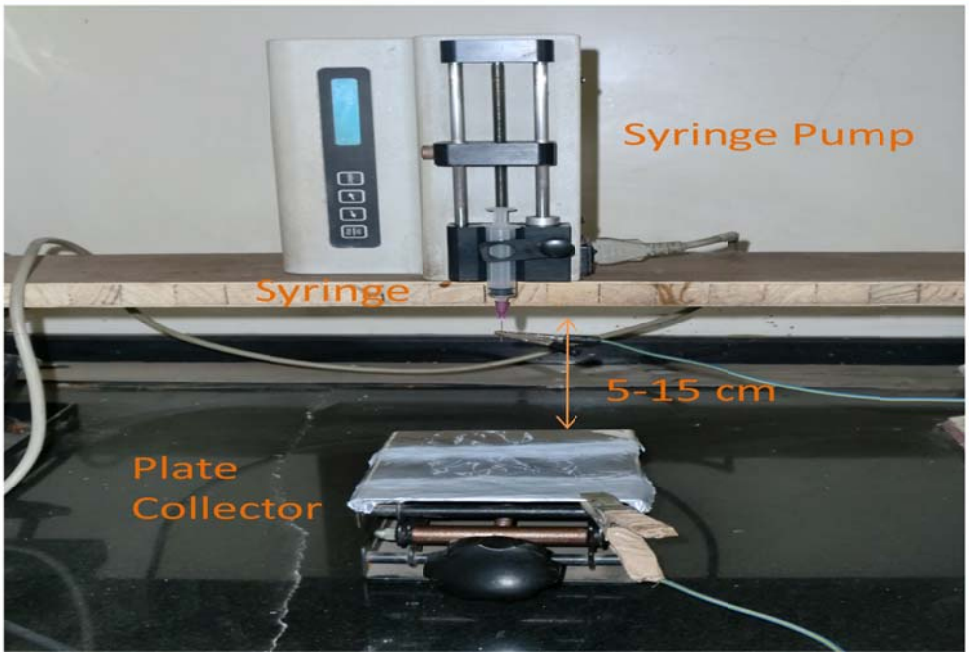

Figure 5.2 Electrospinning Setup Used for Experiment

Table 5.2 Electrospinning Parameters to Produce Aligned Nanofiber varied in the Optimization Tests

Process Parameters	Variables	Fixed Parameters
Collector Design	Air gap metallic strip collector Parallel magnetic collector Patterned collector	22 G flat-tip needle of inner diameter 0.7 mm, Flow rate of 1 ml/hr, Applied voltage of 12 KV, Collector distance of 10 cm and Collecting time of 1 hr
Distance Between Needle Tip and Collector	8 cm 10 cm 12 cm	Flow rate of 1ml/ hr, Applied voltage of 12 KV and Collecting time of 1 hr
Applied Voltage	10 KV 12 KV 14 KV	Flow rate of 1ml/ hr, Collector distance of 10 cm and Collecting time of 1 hr
Flow Rate	1 ml/ hr 2 ml/ hr	Applied voltage of 12 KV, Collector distance of 10 cm and Collecting time of 1 hr

5.3 Modification in collector design to produce aligned nanofibers

5.3.1 Air gap metallic strip collector

Two conductive strips of stainless steel were adjusted to an angle of 60º with each other and placed over the rectangular box which was wrapped by aluminum foil and the whole set up of collector was grounded as shown in figure 4.3. The polymer solution was filled in 10 ml glass syringe fitted with metallic needle of inner diameter of. Then, solution pushed towards tip of needle with the help of syringe pump and on the basis of above experiments, the flow rate was set at 1 ml/ hr with collecting time of 1 hr. After that a high voltage of 12 KV was applied to charge the solution determined from the previous experiments and the distance between collector and the metallic needle was set at 10 cm. After running of electrospinning for 30 seconds, voltage supply was stopped and specimen was taken for analyses under optical microscope for characterization of alignment of fibers. Likewise, experiment was repeated with varied angle between strips, 45º and 60º.

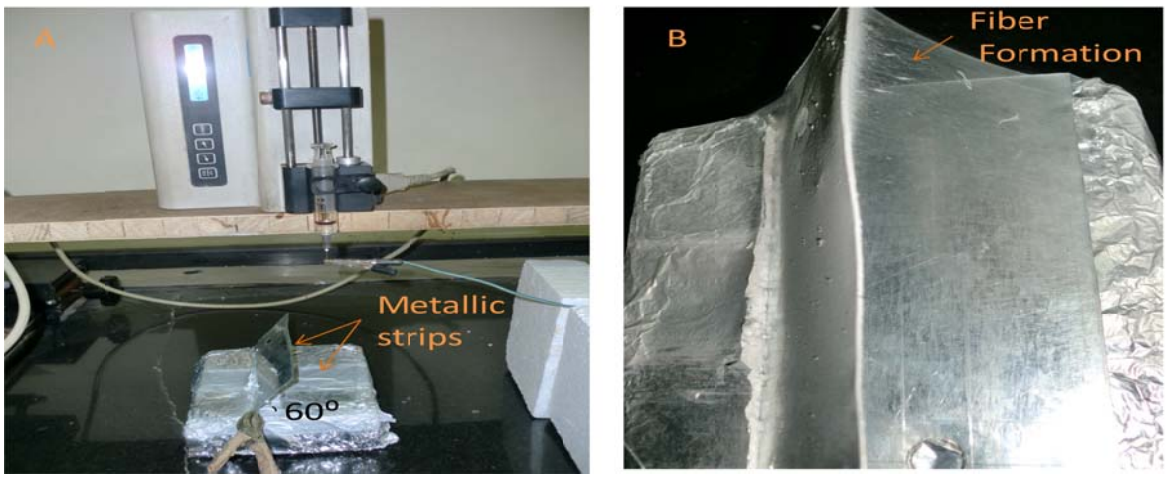

Figure 5.3 (A) The collector consisted of air gap metallic strip at 60º to each other for the collection of aligned nanofibers, (B) Digital photograph of aligned fibers collected between strips

5.3.2 Parallel magnet collector

It is same as conventional electrospinning except the use of ferrite magnets. Due to introduction of magnetic field this technique known as magnetic field assisted electrospinning. In this, two ferrite magnets of surface magnetic field strength of were separated by a gap. The width of gap in this experiment varied from 1cm to 2cm. The PCL solution was loaded into the glass syringe. A constant flow rate of 1 ml/ hr was used to push the solution by using syringe pump. The ferrite magnets were placed at a distance of 10 cm from the tip of needle over the grounded iron plate stage wrapped by aluminum foil as shown in figure 4.4. A voltage of 12 KV was applied between needle and aluminum foil. After that a specimen of fiber was analyzed under optical microscope for the characterization of alignment.

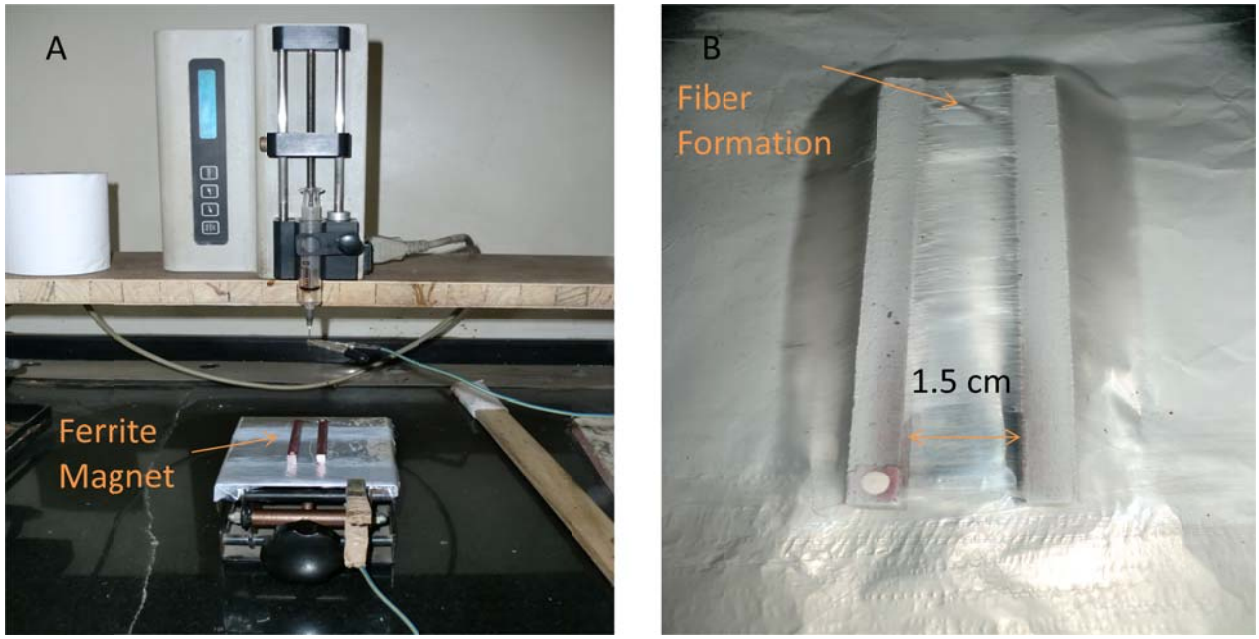

Figure 5.4 (A) The collector consisted of ferrite magnets for the collection of aligned fibers, (B) Digital photograph of aligned fibers collected between parallel magnet collector.

5.3.3 Patterned collector (copper grid collector)

Aligned nanofibers could be produced on the conducting flat plate with the introduction of non conducting gap, get from the works of *Lie et al.* In this, patterned collector were made by soldering of copper conducting wires of different diameters of 2 mm and 3mm into a parallel frames. The width gap between wires varied from 10 mm, 20 mm and 30 mm. Such frame were placed under the tip of needle of distance of 10 cm (distance was also varied from 8 cm to 12 cm to know its effect on alignment), and grounded as shown in figure 4.6. Then, a voltage of 12 KV (varied from 8 – 12 KV) was applied to charge the solution and a flow rate of 1ml/ hr (varied to know its effect) was used to push the solution. Time of deposition for each sample was 30 seconds. After 30 seconds of electrospinning run, specimen of fiber was taken for characterization under optical microscope.

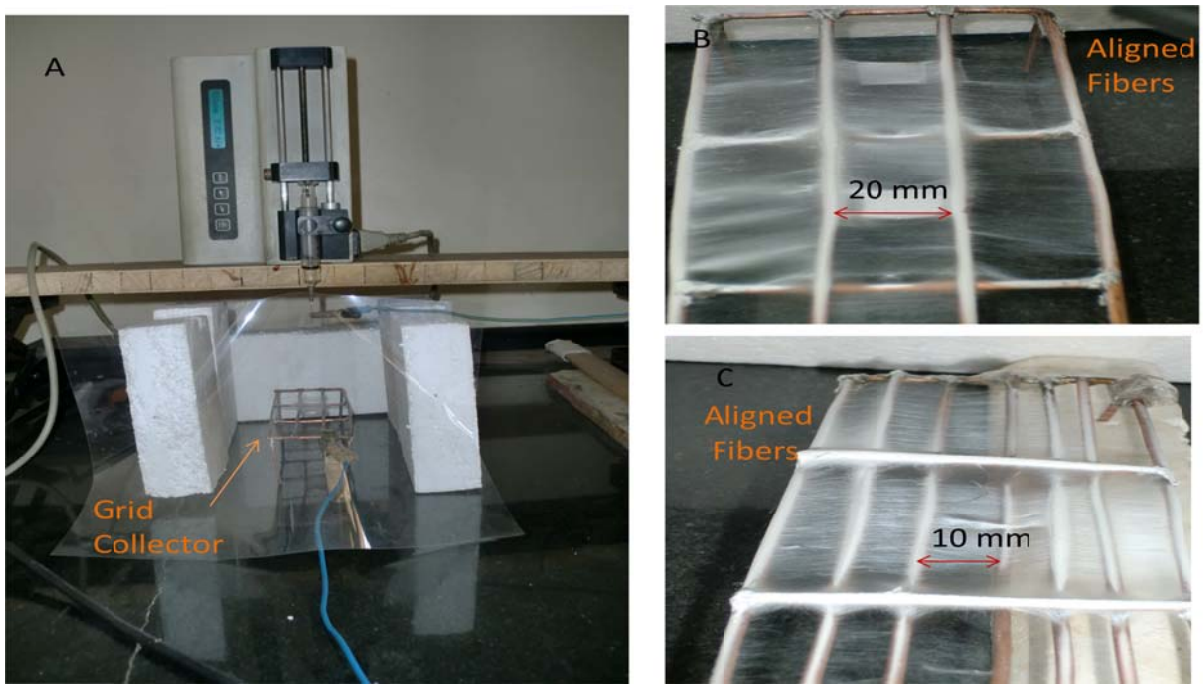

Figure 5.5 (A) Patterned collector consisted of copper wires for the collection of aligned fibers. Digital photograph of aligned fibers collected between wires of width gap (B) 20 mm and, (C) 10 mm.

5.4 Morphological characterization of nanofibrous scaffold

5.4.1 Optical Microscopy and Scanning Electron Microscopy (SEM) Analysis

The morphology and structure of the collected electrospun fibers can be analyzed under optical microscope and scanning electron microscope. A JEOL JSM- 6480LV SEM was used throughout the experiment for characterization of fibers at an accelerating voltage of 15 KV. Samples were prepared by cutting small piece of scaffolds of different electrospinning conditions with the help of scissor. Scaffolds were mounted with the help of carbon tape on the sample holder. Each sample was then coated with a thick layer of platinum by a JEOL JFC -1600 auto fine coater and the operating conditions were 20 mA for 90 seconds.

5.4.2 Quantification of Alignment of Fiber via image analysis using Image J software

Fast Fourier transform (FFT) method was used to quantify the alignment of fibers. In this method original image information converts from the Real space into the mathematical Frequency space through FFT function (34). In this method, a square region of 420 x 420 pixels was selected randomly on SEM micrograph and processed by using Image J software (java version).

5.4.2 Determination of Porosity of Nanofibrous Scaffold

CHAPTER SIX

RESULTS AND DISCUSSION

6. Results and Discussion

6.1 Effect of PCL Concentration on Fiber Morphology and Fiber Diameter

It was observed that the PCL concentration plays major role in fiber morphology and in fiber diameter. No fibers were formed at less than 6wt% PCL concentration for any applied voltage and spinning distance between tip of needle and collector and the reason was that at this concentration, molecular chain entanglement of polymer solution were not sufficient due to the low viscosity of solution which cannot prevent the breakup of the electrically emerged jet and that's why droplets were formed. This can be seen in optical microscopic and SEM micrographs of PCL nanofibers. Figure 6.1 show the fiber morphology obtained at PCL concentration of 6, 8, 10, 12wt% with solvent system of chloroform: methanol at fixed ratio of 3:1 with constant flow rate of 1ml/hr, spinning distance of 10cm, an applied voltage of 12 KV and constant room temperature and relative humidity of 42-50%. At 8 wt% concentration less than 400 nm fibers diameter were obtained with beads over the mesh and also the fiber volume was less and fibers were not uniform (figure 6.1a). At 10 wt% concentration fibers diameter obtained were more than 400nm but fibers were bead free and uniform and continuous. Continuous but not uniform fibers were obtained above the 12 wt% without consideration of applied voltage and spinning distance and the reason was that the PCL solution has sufficient molecular chain entanglement which can prevent the breakup of emerged jet and under influence of electrostatic forces which further elongate the jet to form fibers but the average diameter was much larger than that of lower concentrations. And the requirement of the experiment was to obtain smaller fiber diameter with uniformity and continuity and that obtained at 10 wt%. On the basis of the result it was concluded that on increase in concentration there is increase in viscosity of solution. Table 5.1 shows a summary of the formation of fiber at different polymer concentration. The average

diameter obtained was 455.33 nm. The distribution of fiber diameters at 8, 10 and 12 wt% concentration is shown in Figure 6.2 and Figures 6.3 and Table 6.2 summarize the diameter distribution. The SEM micrograph in figure 6.4 shows the measured fiber diameter at 10 wt% concentration in chloroform: methanol.

Table 6.1 Dependence of fiber morphology on PCL concentration

Concentration by weight	Fiber Morphology
6	No fiber
8	Fibers with beads
10	Uniform continuous fiber
12	Continuous but not uniform fibers

Table 6.2 The diameter of fiber at 8, 10 and 12 wt% concentration of PCL

Polymer Concentration (%)	Diameter of fiber (nm)		
8	STDV: 24.28	Max: 401	Min: 340
10	STDV: 44.45	Max: 470	Min: 369
12	STDV: 138.46	Max: 833	Min: 601

Table 6.3 Dependence of Fiber Morphology on Different Solvent System

Solvent System	Fiber Morphology
Chloroform: Methanol	Branched Fibers and non uniform
Di-chloromethane : Di-methylformamide	Fibers with bead, non-uniform and discontinuous
Chloroform + Di-chloromethane : Di-methylformamide	Bead free, uniform and continuous

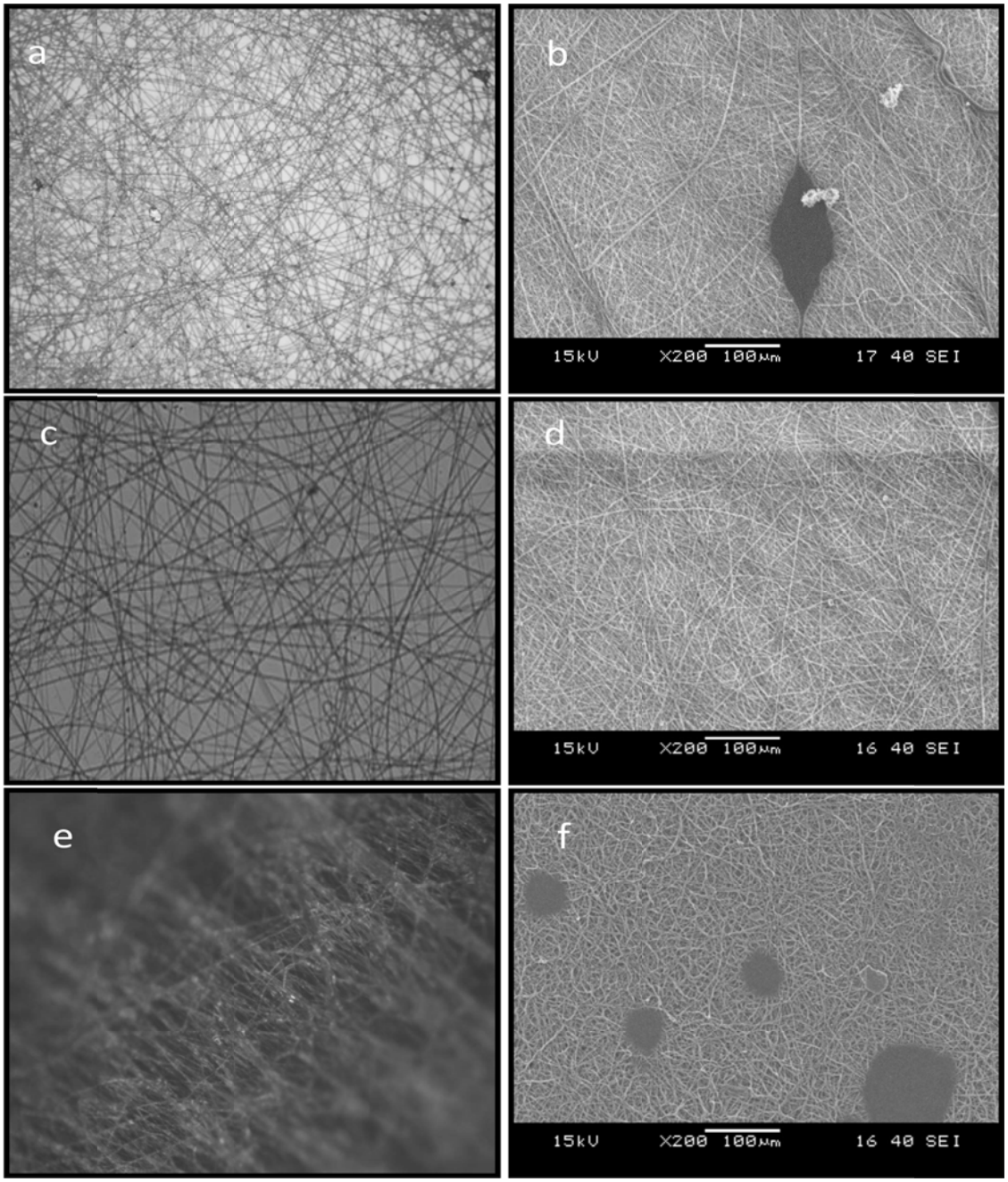

Figures 6.1- Optical Microscope Micrographs at 10X and SEM Micrographs at 200X. The morphology of fibers at 8 wt% (a, b), 10 wt% (c, d) and 12 wt% (e, f) with constant flow rate of 1ml/hr, an applied voltage of 12 KV and spinning distance of 10 cm.

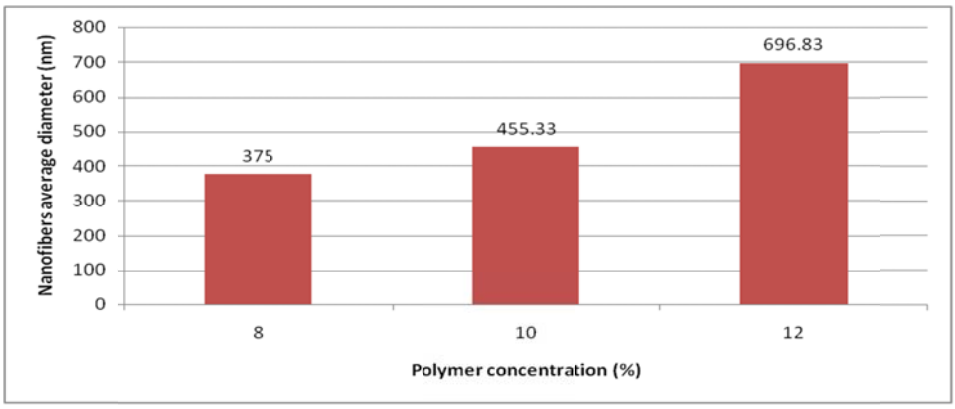

Figures 6.2 Average nanofibers diameter obtained at 8, 10, and 12 wt% concentration PCL with chloroform + dichloro methane: dimethyl formamide in 3:1 ratio at 12 KV voltage, spinning distance of 10 cm and flow rate of 1 ml/hr

8 wt%-12 KV-10 cm- 1ml/hr

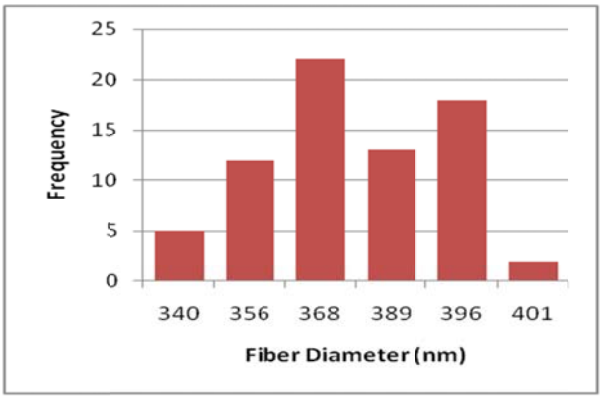

12 wt%- 12 KV- 10 cm- 1ml/hr

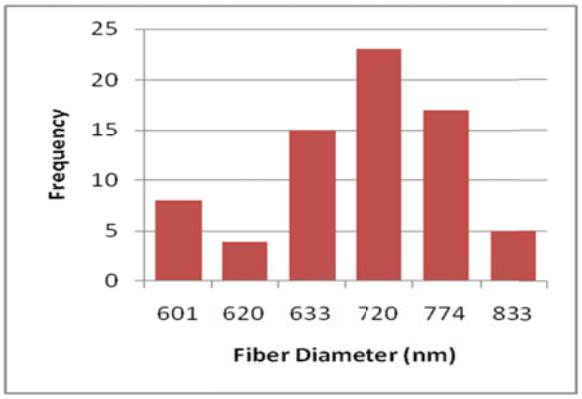

10 wt%- 12 KV- 10 cm- 1ml/ hr

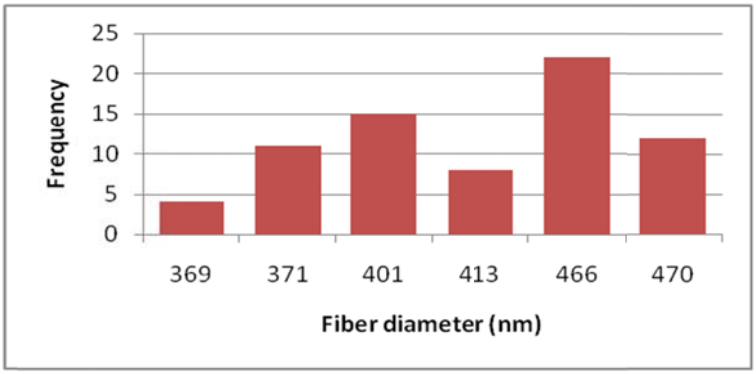

Figures 6.3 The fibers diameter distribution at concentration of 8, 10, and 12 wt% with constant 12 KV voltage and spinning distance of 10 cm.

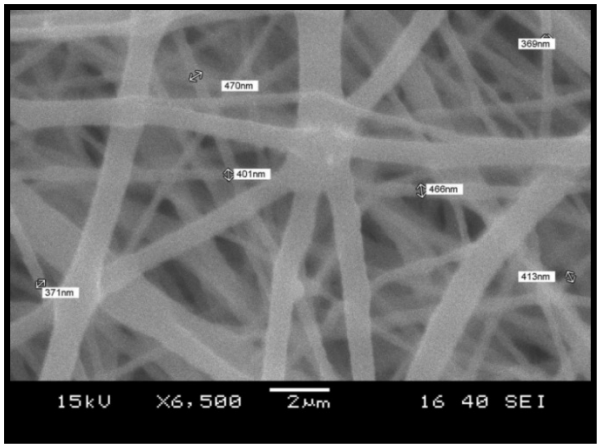

Figure 6.4 SEM micrograph of 10 wt% PCL solution at 12 KV with constant spinning distance of 10 cm shows the measured fiber diameter on scale bar of 2 µm.

6.2 Effect of Solvent System on Fiber Morphology and Fiber Diameter

It was observed that the solvent system used to prepare PCL solution plays an important role in fiber morphology and on fiber diameter. Figure 6.5 shows the fiber morphology obtained from different four solvent systems: chloroform: methanol, dichloro methane: dimethyl formamide, chloroform + dichloro methane: dimethyl formamide and chloroform: dimethyl formamide, those were used for preparation of 10 wt% concentration of PCL and electrospun at constant flow rate of 1 ml/hr, spinning distance of 10 cm and an applied voltage of 12 KV. From the SEM micrograph, it was depicted that the solvent system of chloroform + dichloro methane: dimethyl formamide produced fibers were more uniform in comparison to other solvent system and the reason was the low dielectric constant of dichloro methane and on addition of chloroform in equal amount in 3:1 ratio with dimethyl formamide was found to be enhanced the spinning process and uniformity. From figure 6.6, it was observed that there was slight difference in the diameter of fibers of different solvent system. The small fiber diameter was obtained with the chloroform + dichloro methane: dimethyl formamide. The average diameter of fibers obtained was 397 nm. Table 6.3 summarized the fiber morphology at different solvent system.

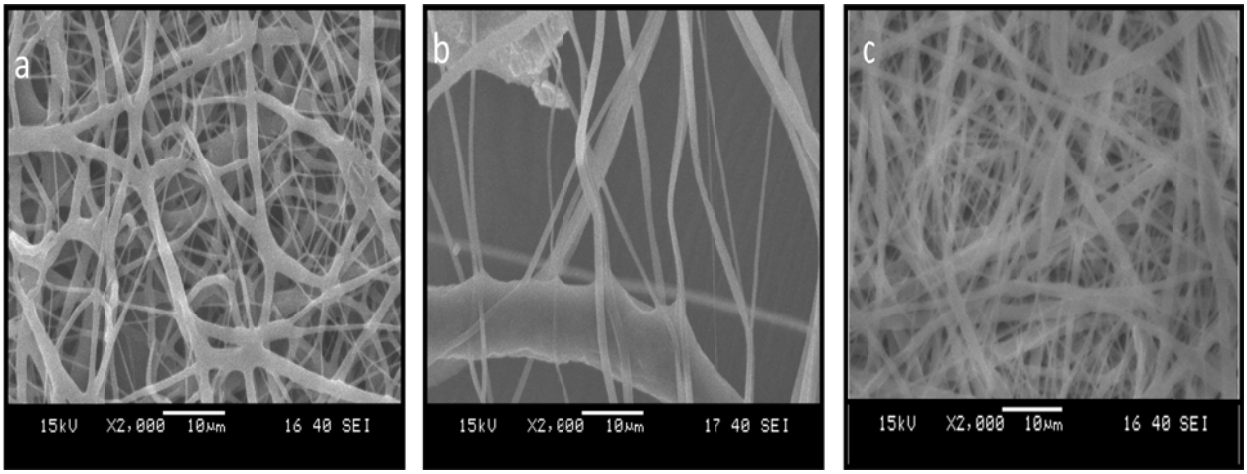

Figures 6.5 SEM Micrographs of 10 wt% PCL in 3:1 solvent ratio of solvent system (a) chloroform: methanol, (b) dichloro methane: dimethyl formamide, (c) chloroform+ dichloro methane: dimethyl formamide.

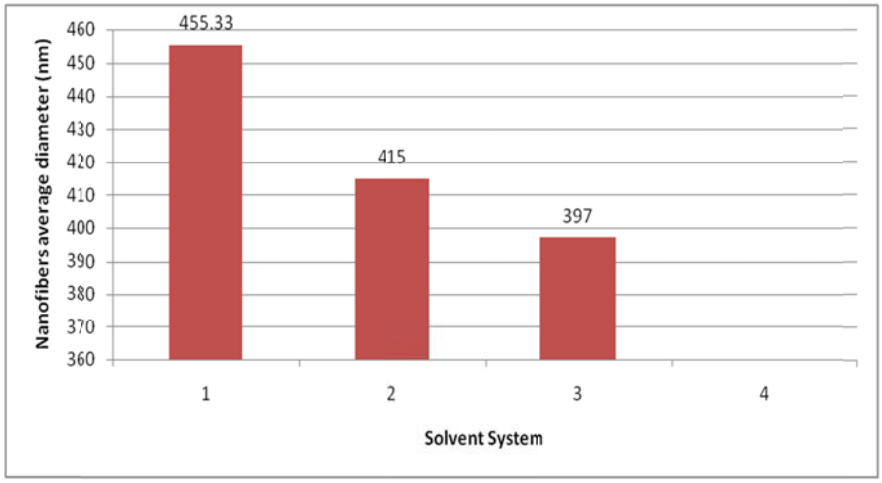

Figure 6.6 Distribution of Average fiber diameter at different solvent system. 1) Chloroform: methanol; 2) Dichloro methane: dimethyl formamide; 3) Chloroform + dichloro methane: dimethyl formamide.

6.3 Effect of Solvent Ratios on Fiber Morphology

It was observed that the ratios of solvent have great influence on the fiber morphology. Figures 6.7 shows the optical micrographs of different solvent ratios 1:1, 2:1, 3:1, 4:1 and 5:1 of the solvent system: chloroform + dichloro methane: dimethyl formamide which were used to prepare

10 wt% concentration and electrospun at a flow rate of 1 ml/hr, spinning distance of 10 cm and an applied voltage of 12 KV. It was observed from these micrographs that the fibers obtained at 1:1 solvent ratio that is at low concentration of chloroform and dichloro methane were fragile, broke easily and lack of uniformity. Where, when there was large quantity of chloroform and dichloro methane in the solution (5:1), the diameter of fibers obtained were large as compared to 1:1 solutions and this caused the formation of bead but the fibers obtained were continuous as seen in the Figure 6.6 (e). Table 6.4 summarizes the effect of all solvent ratios on fiber morphology and on fiber diameter. Based on the micrographs and fiber diameter comparison it was decided that the most suitable ratio to prepare solution for electrospinning was 3:1 and the reason was, fiber diameter, consistency, continuity and uniformity of fibers.

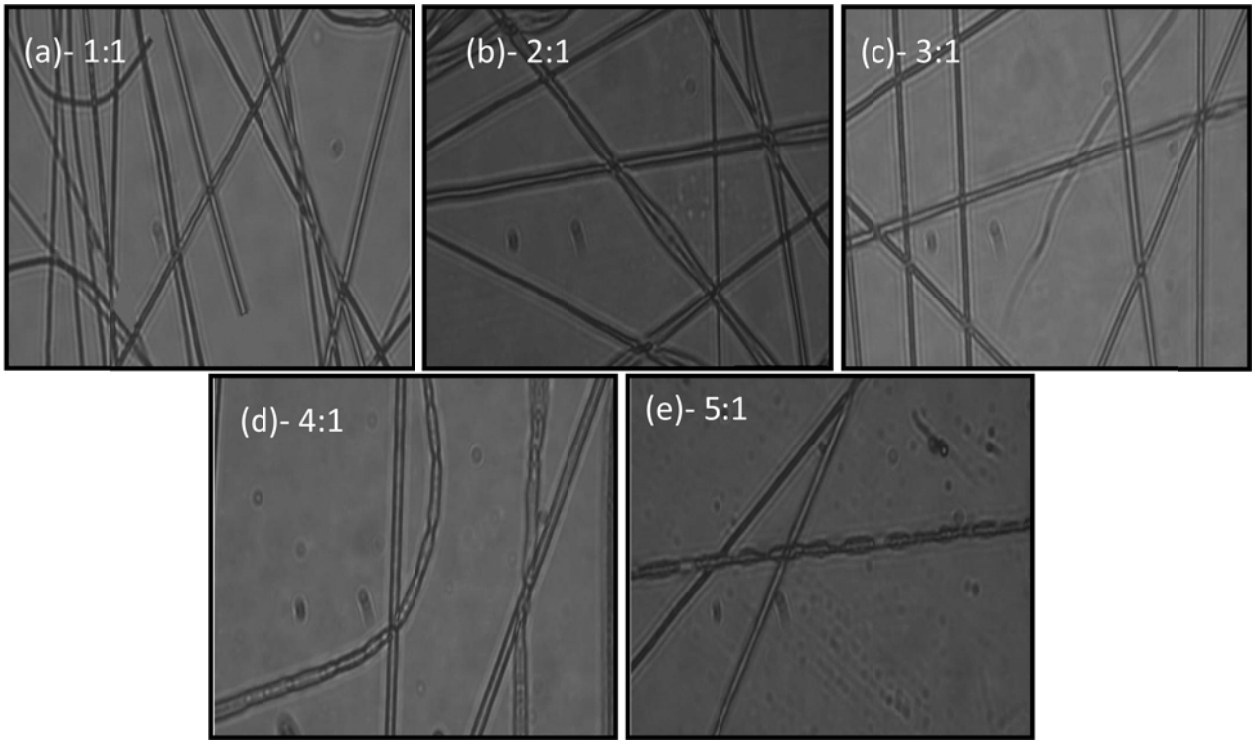

Figures 6.7 The optical micrographs of 10 wt% PCL in different solvent ratios (a) 1:1, (b) 2:1, (c) 3:1, (d) 4:1 and (e) 5:1

Table 6.4 Fiber Morphology obtained for each Solvent Ratio

Solvent Ratio	Fiber Morphology
1:1	Broken fibers with non uniformity
2:1	Non-uniform fibers
3:1	Uniform and continuous fibers with very less beads
4:1	Fibers with beads
5:1	Large number of beads on fibers

6.4 Effect of Applied Voltage on Fiber Morphology and Fiber Diameter

After optimization of solution parameters, the process parameters were optimized and studied their effect on fiber morphology and on fiber diameter. Figure 6.8 shows SEM micrographs and it was observed from both the micrographs that the fibers obtained at conditions of 8 KV voltage and spinning distance of 10cm were not uniform and fibers were not totally dried and the reason was, as the distance between collector and needle tip decreases the time requires for drying up of fibers get reduces and without drying fibers get deposits on collector plate as seen in Figure 6.8(a). When voltage was increased to 14 KV and the spinning distance was same at 10 cm, at this conditions, it was found that the fibers were still non-uniform and formation of beads on the woven fibers and the reason was, when voltage is above the critical value before formation of Taylor cone the electrostatic forces causes drops to drip, it can be seen in Figure 6.8 (b). Figure 6.9 shows the relationship between average fiber diameters, applied voltages (10, 12, and 14 KV) and spinning distances (8, 10, and 12 cm) of 10 wt% PCL solution in chloroform + dichloro methane: dimethyl formamide in 3:1 ratio. It was found that the lesser fiber diameter was obtained at 14 KV and 12 cm, but according to graphs morphology fibers were not good. At 10 KV and 10 cm larger fiber diameter were obtained which was not the need for this experiment.

So, the most appropriate condition to produce uniform, continuous with small fiber diameter was 12 KV and 10 cm spinning distance.

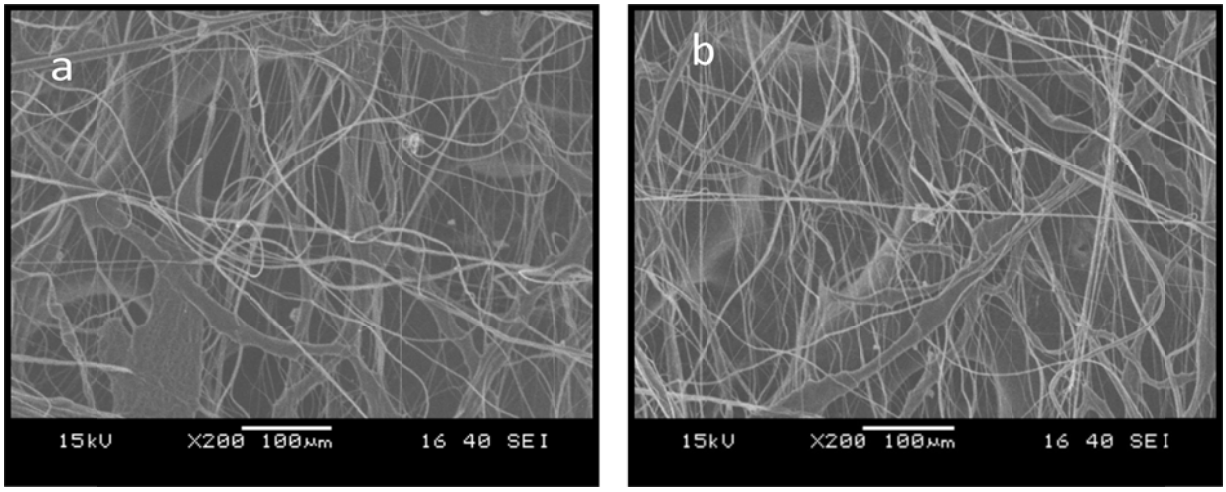

Figures 6.8 SEM micrograph of 10 wt% PCL in 3:1 solvent (chloroform+ dichloro methane: dimethyl formamide) ratio solution. (a) at 10 KV voltage and spinning distance of 10 cm, (b) at 14 KV and spinning distance of 10 cm

Table 6.5 Summary of Fiber Morphology at Different Applied Voltage

Applied Voltage (kV)	Fiber Morphology
8	Broken fibers, more number of beads, discontinuity
12	Uniform fibers and continuous
14	Non-Uniform and continuous fibers with very less beads

5.5 Effect of Flow Rate on Fiber Morphology and Fiber Diameter

It was observed from the SEM micrographs as shown in Figure 6.10 that the fibers at 1 ml/hr as shown in figure 6.10(a) were more uniform and continuous in comparison to the flow rate of 2 ml/hr which can be seen in figure 6.10 (b), where fibers get clumped and there was no uniformity in fibers and the reason was, fibers did not get sufficient time to dry before reaching to the plate

collector. Figure 6.11 shows the distribution of fibers at different flow rates and from that it was inferred that at 1ml/hr, small fiber diameter (360-470 nm) was obtained as compared to 2 ml/hr where the diameter of fiber was ranges from 600- 850 nm. The average diameter obtained at flow rate of 1 ml/hr was 397 nm.

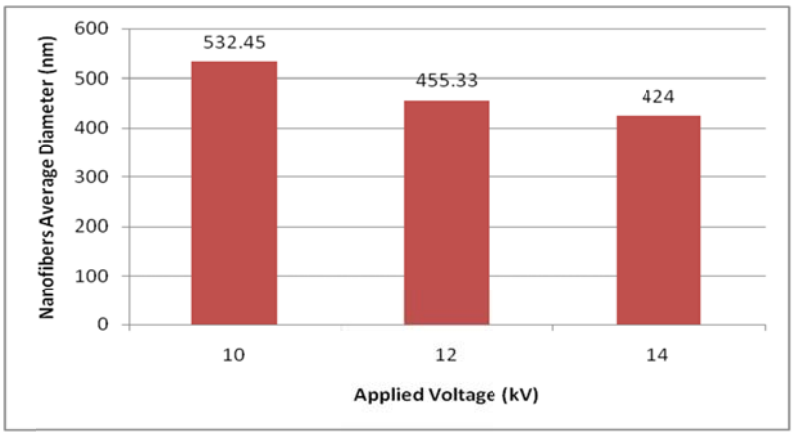

Figures 6.9 The relationship between average fiber diameter, applied voltage (10, 12, and 14 KV) and spinning distance (8, 10, and 12 cm) of 10 wt% PCL.

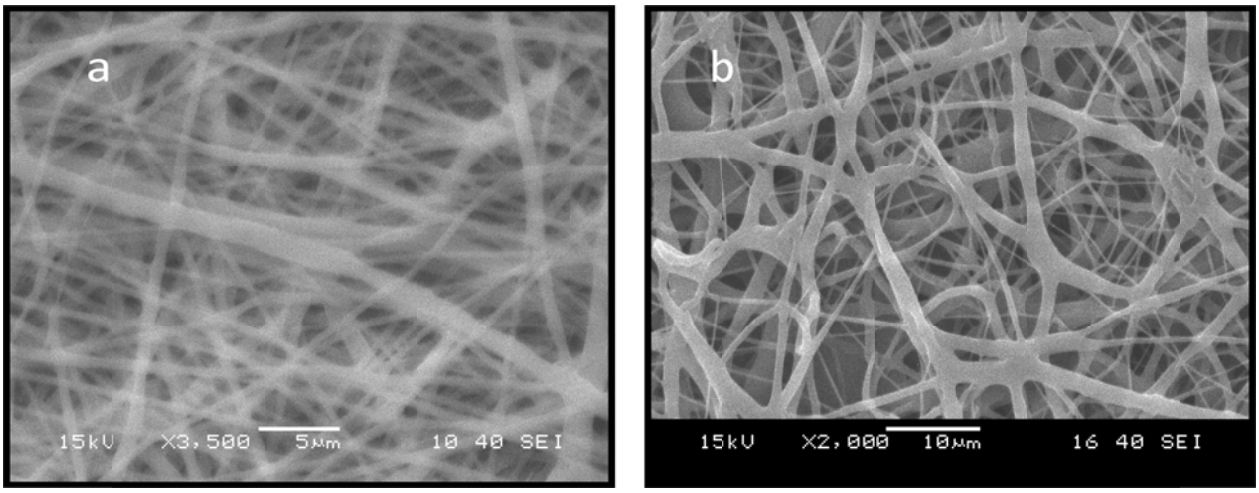

Figures 6.10 The SEM micrograph of 10 wt% PCL solution at flow rate of (a) 1 ml/hr at 3500X and (b) 2 ml/hr at 2000X.

Table 6.6 Summary of Fiber Morphology at Different Flow Rates

Flow Rate (ml/hr)	Fiber Morphology
1	Uniform and Continuous
2	Branched fibers

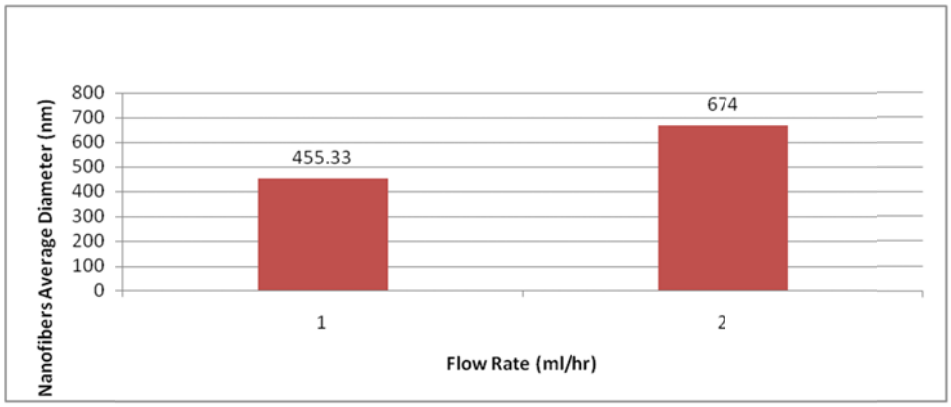

Figures 6.11 The distribution of fiber diameter at different flow rates.

6.6 Optimized Electrospinning Conditions

The effect of each of these solution parameters (polymer concentration, solvent system and solvent ratio) and process parameters (applied voltage, distance between needle tip and collector and flow rate) were studied and experimented to produced uniform, continuous fibers with nano-range diameter. And according to the results the optimized conditions that obtained after so many trials produced PCL uniform, continuous nanofibers of diameter which ranges from 360-470 nm illustrated in Table 6.5.

All experimental trials had been done using plate collector, produced random nanofibers at above stated optimized conditions at constant room temperature and relative humidity of 48-52%. The optimized solution further used for optimization of collectors design for aligned nanofibers.

Table 6.5 Optimized Conditions for Electrospinning Process

Electrospinning Parameters	**Optimized Parameters**
Solution Parameters	
Polymer Concentration	10 wt%
Solvent System	Chloroform+ Dichloro methane: Dimethyl formamide
Solvent Ratio	3:1
Process Parameters	
Applied Voltage	12 KV
Spinning Distance	10 cm
Flow Rate	1 ml/hr

6.7 COLLECTOR MODIFICATION

6.7.1 Air Gap Metallic Strip Collector

6.7.1.1 Effect of Angle between the Strips on Fiber Alignment and Fiber Diameter

The effect of gap between metallic strips in air gap metallic strip collector was studied at 60° and 45° angle. SEM images in Figure 6.12(a, b and d, e), FFT output image in Figure 6.12(c and f) demonstrate the alignment of the fibers. The narrower areas of central parts in FFT output images indicate alignment of fiber and from figures 6.12(c and d), it was observed that the area was narrower at 45°, that means fibers were more aligned at 45° than 60° and the reason was decrease in the gap between two strips due to decrease in angle and the residual electrostatic force which repels the spun fiber is more in the vicinity of electrode which causes fibers to attached to the electrodes in an alternate fashion as seen figure 4.3 (b) and collected as array of

aligned fibers.. Where figure 6.12 shows partial alignment of fiber using this collector. The average diameters of nanofibers obtained were 448 nm at 45° and 460 nm at 12 KV.

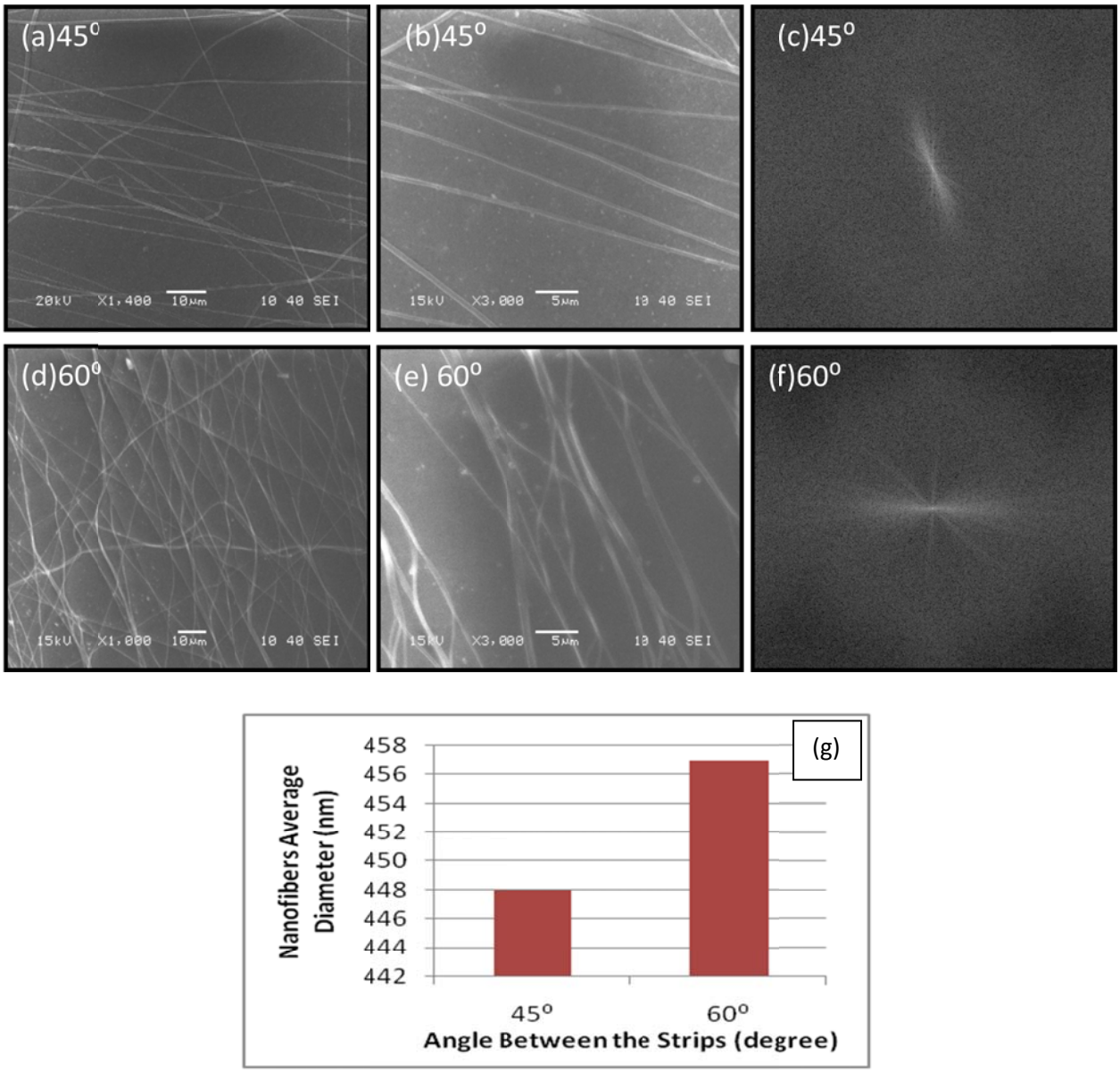

Figures 6.12 The SEM micrographs of PCL nanofibers collected at different angles between air gap metallic strips. SEM images of fibers collected at (a, b) 45°, and (d, e) 60°. (c and f) FFT images from 420X420 pixel selection from (a, d) images respectively, (g) Plot of average fiber diameter collected under different angles. SEM images magnification are 1000X, 1400X and 3000X.

6.7.1.2 Effect of Applied Voltage and Spinning Distance on Fiber Alignment

The effect of applied voltage of 10, 12, and 14 KV and spinning distance of 8, 10, and 12 cm were studied. It was observed from the optical images as shown in figures 6.13 (a-c) that at 14 KV more number of crossing fibers were more as compared to 10 and 12 KV, whereas at 10 KV minimum number of crossing fibers were observed. The reason behind this was, on increasing the voltage, more branching of nanofibers will occur and that creates problem in alignment across the gap. Optical images in figure 6.13 (d-f) demonstrate that on increasing the spinning distance, the number of aligned fibers and broken fibers increases. So, on the basis of experimental trials most appropriate conditions that produced aligned fibers were 12 KV voltage and 10 cm spinning distance.

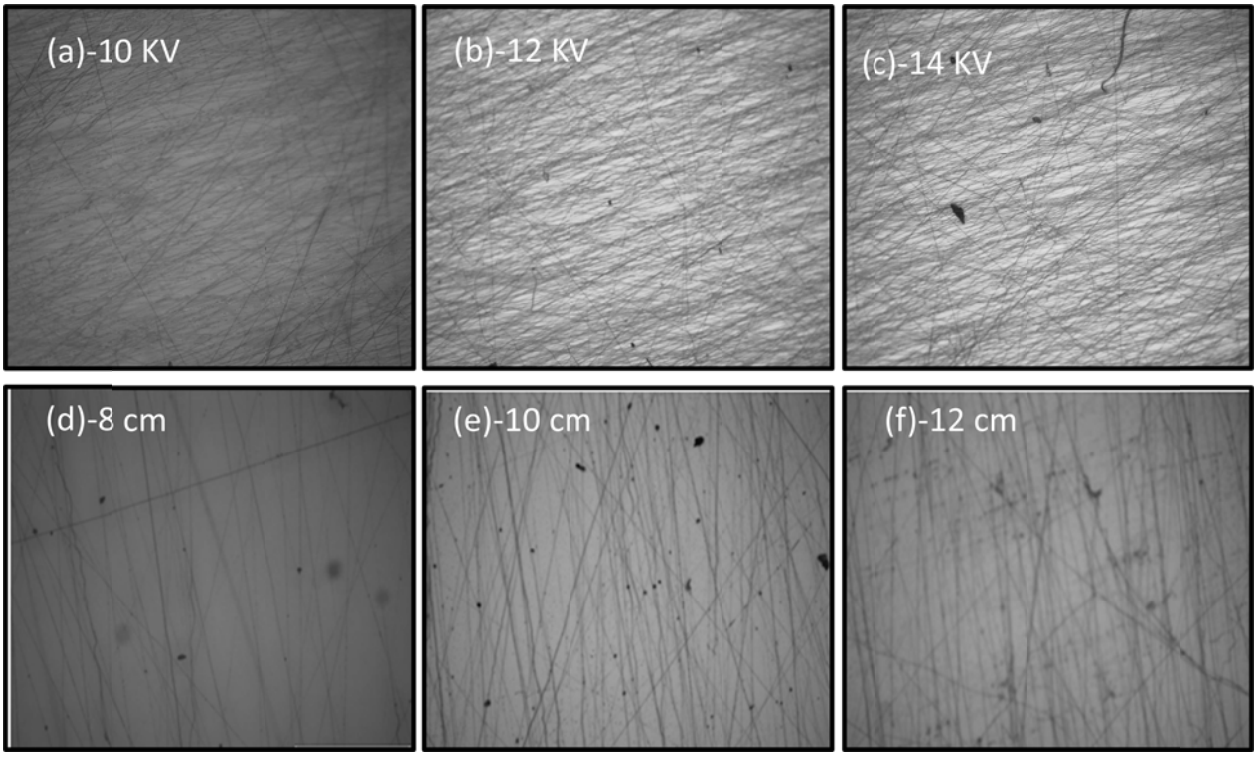

Figures-6.13 Optical images of nanofibers at different applied voltages and spinning distances. (a-c) Optical images of fibers collected at 10KV (a), 12 KV (b), and 14 KV (c). (d-f) Optical images of fibers collected at 8 cm (d), 10 cm (e), and 12 cm (f).

6.7.2 Parallel Magnet Collector

6.7.2.1 Effect of Gap Width between Magnets on Fiber Alignment and Fiber Diameter

The effect of using magnets in place of conducting metal was studied at different gap distance between magnets of 1.5 cm and 2 cm. SEM images as shown in Figure 6.14 (a-c) and FFT output image in Figure 5.13 (d) shows the alignment of fiber. On comparison of FFT output images at different widths, it was found that central part area was narrower in figure 6.14 (c) in comparison to figure 6.14 (f) and the reason was, the introduction of magnetic field superimposes the electrostatic forces and balance off the forces those creates instability and decreases the chances of formation of branched fibers. Figure 6.14 shows improved alignment with decreased gap widths. Alignment of fibers obtained with magnet collector was better than metallic strip collector. The average fiber diameter obtained was 499.

6.7.2.2 Effect of Applied Voltage and Spinning Distance on Fiber Alignment

The effect of applied voltage of 10, 12, and 14 KV and spinning distance of 8, 10, and 12 cm were studied in this experiment. It was observed from the optical images as shown in figures 6.15 (a-c) that web and wavy like structure were formed with increased voltage. Optical images in figure 6.15 (d-f) demonstrate that on increasing the spinning distance, the number of aligned fibers and broken fibers increases. So, on the basis of experimental trials most appropriate conditions that produced aligned fiber was 12 KV voltage and 10 cm spinning distance. The average diameter obtained was 499. It was found that, the flow rate does not have any profound effect on fiber alignment but it does have effect on the fiber diameter.

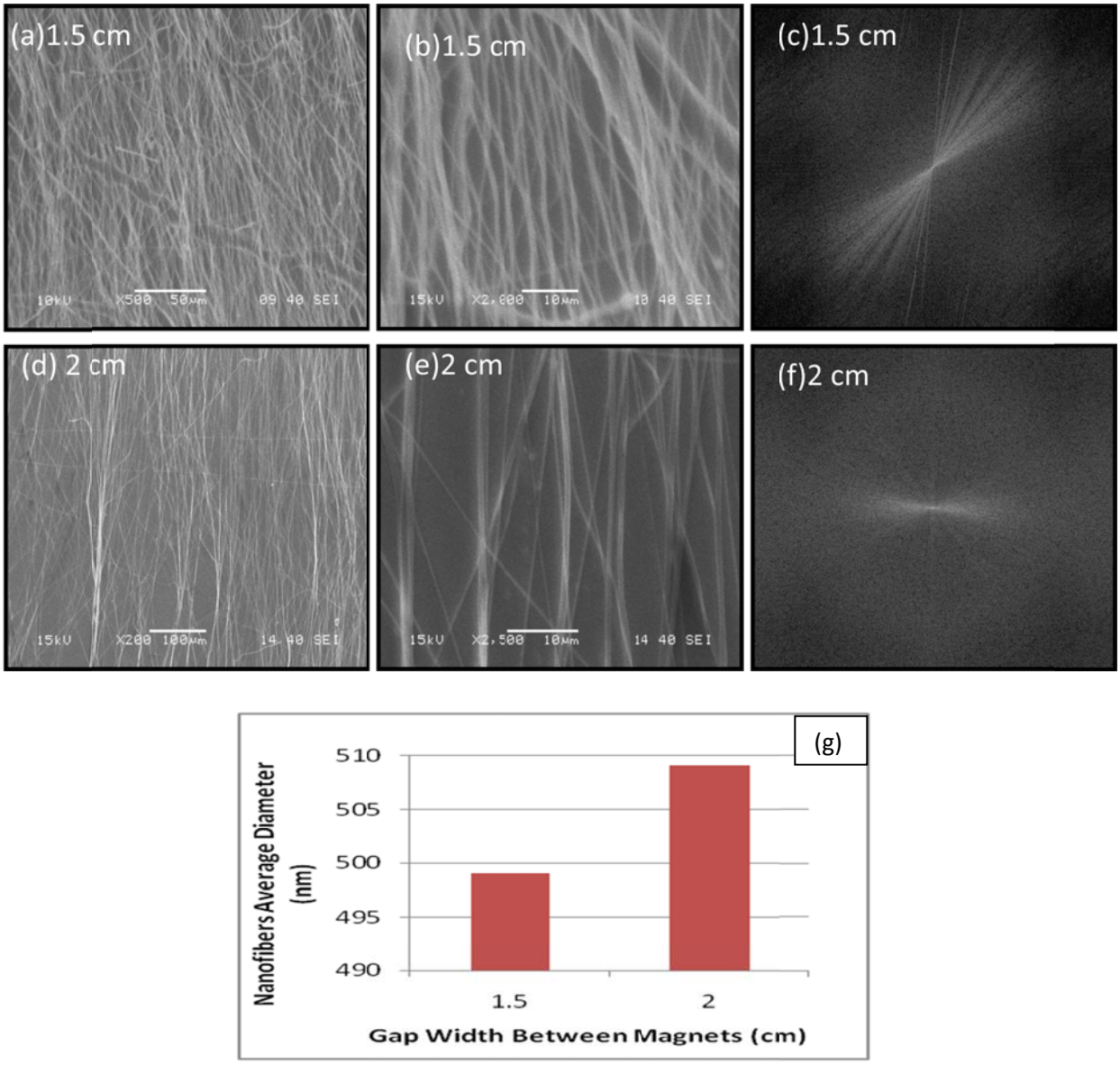

Figure 6.14 The SEM images of PCL fibers collected on Parallel magnet collect at different gap width. (a, b) SEM images of fibers collected at (a, b) 1 cm, and (d, e) 2 cm. (c and f) FFT images from 420X420 pixel selection from (a, d) images, respectively. (g) Plot of average fiber diameter collected under different width gaps. SEM images magnification are 200X, 500X, 100X and 2500X.

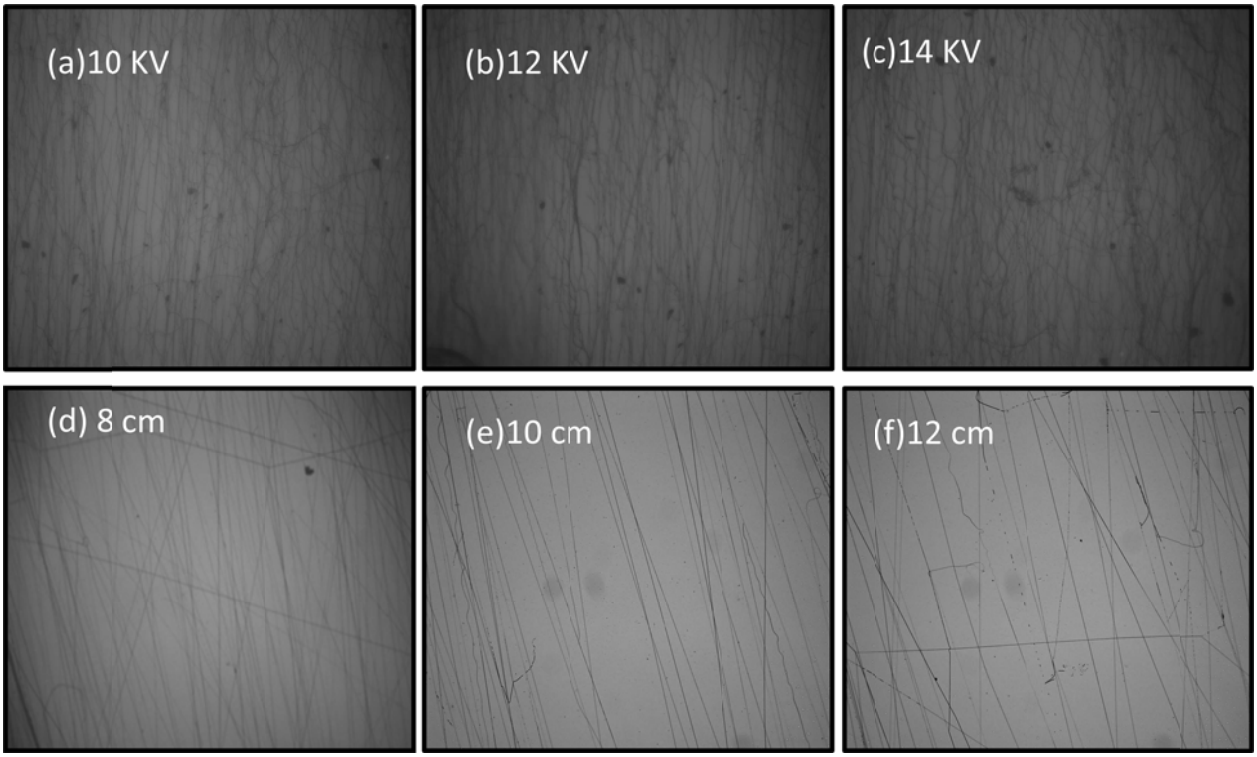

Figures-6.15 Optical images of nanofibers at different applied voltages and spinning distances. (a-c) Optical images of fibers collected at 10KV (a), 12 KV (b), and 14 KV (c). (d-f) Optical images of fibers collected at 8 cm (d), 10 cm (e), and 12 cm (f).

6.7.3 Patterned Copper Grid Collector

6.7.3.1 Effect of Gap Width between Wires on Fiber Alignment and Fiber Diameter

The copper grid collector of 1 cm and 2 cm width gap was used to study the effect of varying gap on fiber alignment. It was hypothesized that more the number of wires, minimum the width gap between them. SEM images figure 6.16 (a, b) and figure 5.15 (d, e) and FFT output images figure 6.16 (c) and figure 6.16 (f) demonstrate the fiber alignment. The central part was narrow in 1 cm gap width as compared 2 cm, and compare to other collectors this collector shows the narrowest area of center part which indicate the improved fiber alignment with 1 cm gap width and the reason behind this was, the wires were closer to each other and obtained high transversal electrostatic forces across the gap which drawn fibers from one wire to other in alternate fashion

and produced aligned array of fibers. The highly aligned fibers obtained from using copper patterned grid collector of 1 cm gap width. The average diameter obtained was 447.

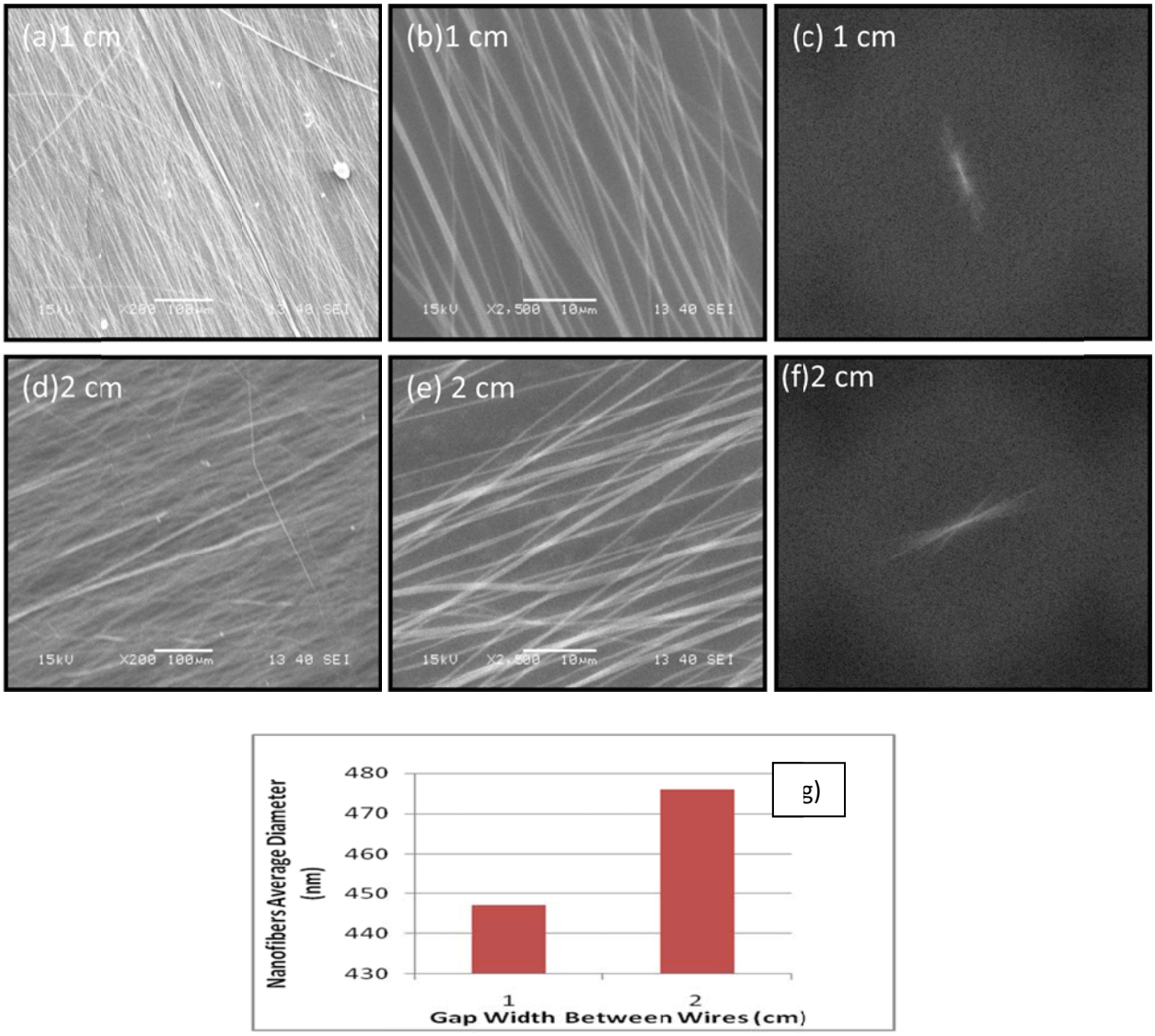

Figure 6.16 The SEM images of PCL fibers collected on Patterned copper grid collector at different gap width. (a, b) SEM images of fibers collected at (a, b) 1 cm, and (d, e) 2 cm. (c and f) FFT images from 420X420 pixel selection from (a, d) images, respectively. (g) Plot of average fiber diameter collected under different width gaps. SEM images magnification are 200X, and 2500X.

6.7.3.2 Effect of Applied Voltage and Spinning Distance on Fiber alignment

The effect of applied voltage and spinning distance were studied at 10, 12, and 14 KV and 8, 10, and 12 cm. It was observed from the optical images as shown in figures 6.17 (a-c) that, the alignment of fiber was good at 12 KV in comparison to 10 and 14 KV. At 14 KV, the degree of alignment was high and as the voltage decreased degree of alignment was decreased. Most aligned fiber was obtained at 10 KV but the fiber morphology was not good. Beads were formed along fibers. Optical images in figure 6.17 (d-f) demonstrate the effect of spinning distance on alignment and it was observed that, on increasing the spinning distance, the number of aligned fibers and broken fibers increases and at low distance clumping of fibers were observed.

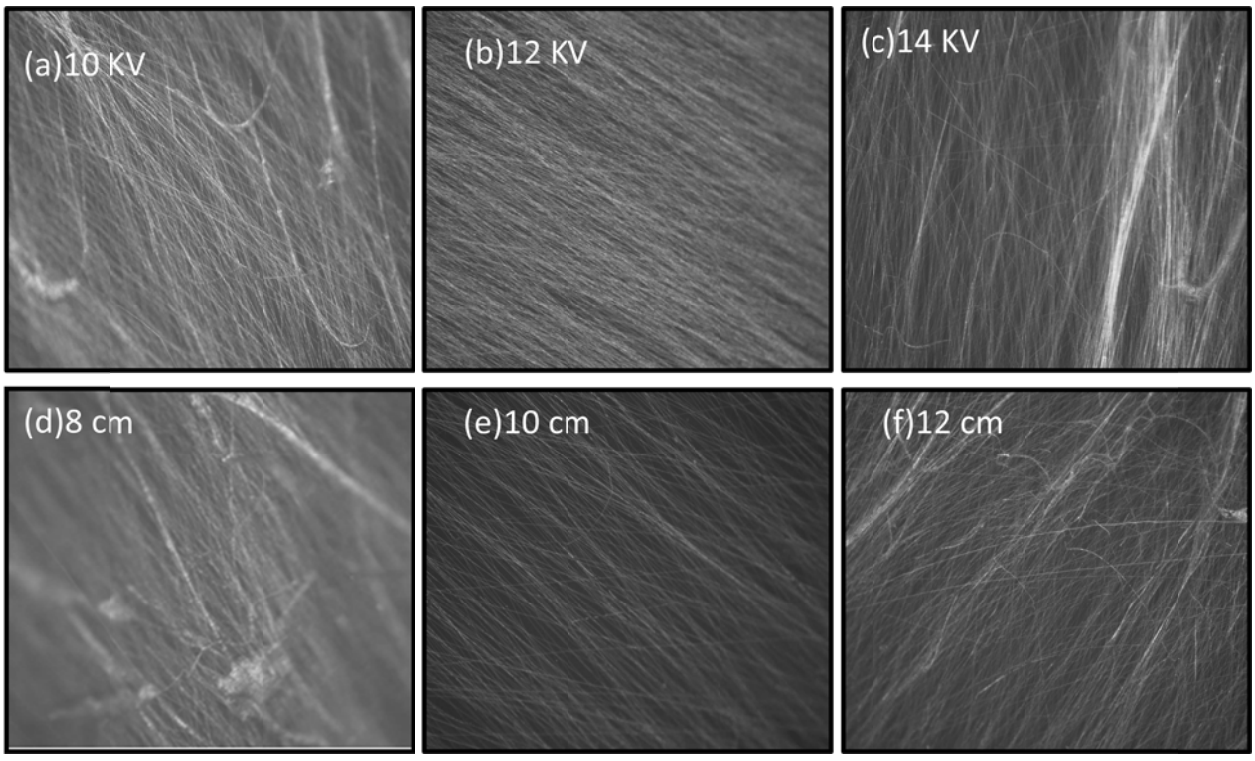

Figures-6.17 The optical images of nanofibers at different applied voltages and spinning distances. (a-c) Optical images of fibers collected at 10KV (a), 12 KV (b), and 14 KV (c). (d-f) Optical images of fibers collected at 8 cm (d), 10 cm (e), and 12 cm (f).

CHAPTER SEVEN

CONCLUSION

6. Conclusion

This research work demonstrated the possibility of creating highly aligned nanofibers of PCL by manipulating the parameters of electrospinning method. These parameters govern the whole process of electrospinning and on manipulation, effect the morphology and orientation of fibers. On analyzing the results obtained from optical microscopic and SEM analysis can lead to a conclusion that, in the current project, uniform, continuous and aligned fibers with nano-range fiber diameter were successfully obtained by manipulating the solution parameters, process parameters and the design of collectors in electrospinning process. The optimized conditions of electrospinning process that produced bead free fibers with uniformity and continuity were PCL concentration of 10% (w/w), spinning distance of 10 cm, a flow rate of 1 ml/hr and an applied voltage of 12 kV. The solvent system mix of chloroform+ dichloro methane: dimethyl formamide of 3:1 ratio was proved to be the best combination for uniformity and continuity of fibers. The general morphology showed a range of fibers diameters in random fibers were 350 to 480 nm at these optimized conditions. But, according to literature random fibers is not as efficient as aligned fibers to promote the growth and differentiation of neural cells and also the cross fibers on random mat may divert the direction or stop the extension of neurites. The optimized solution further used to fabricate aligned nanofibers. Different collectors were fabricated as the design of collectors is the most influential factor to produce aligned nanofibers. SEM and optical microscope micrograph showed that the best fiber alignment was obtained from copper grid patterned collector at optimal conditions of electrospinning established previously.

Thus it can be concluded that the electrospinning process made it possible to fabricate PCL aligned nanofibrous scaffold that is critical to neuronal cell growth and regeneration.

CHAPTER EIGHT

REFERENCES

8. REFERENCES

1. Lee Y S and Arinzeh T L. Electrospun Nanofibrous Materials for Neural Tissue Engineering. *Polymers* 2011; **3:**413-426.
2. Kim Y T, Haftel V K, Kumar S and Bellamkonda R V. The role of aligned polymer fiber-based constructs in the bridging of long peripheral nerve gaps. *Biomaterials* 2008; 29**:**3117–27.
3. Orive G, Anitua E, Pedraz J L, Emerich D F. Biomaterials for promoting brain protection, repair and regeneration. *Nat. Rev. Neurosci.* 2009; **10:**682-692.
4. Ma Z, Kotaki M, Inai R and Ramakrishna S. Potential of nanofiber matrix as tissue-engineering scaffolds *Tissue Eng.* 2005; **11:**101-109.
5. Li WJ, Laurencin CT, Caterson EJ, Tuan RS and Ko FK. Electrospun nanofibrous structure: a novel scaffold for tissue engineering. *J Biomed Mater Res* 2002; **60:**613–21.
6. Cai J, Peng X, Nelson K D, Eberhard R and Smith G M. Permeable guidance channels containing microfilament scaffolds enhance axon growth and maturation. *J. Biomed. Mater. Res. A* 2005; **75:**374–86.
7. Chen M, Patra PK, Warner SB and Bhowmick S. Optimization of electrospinning process parameters for tissue engineering scaffolds. *Biophys Rev Lett* 2006; **1:**153–78.
8. Li WJ, Laurencin CT, Caterson EJ, Tuan RS, Ko FK. Electrospun nanofibrous structure: a novel scaffold for tissue engineering. *J Biomed Mater Res* 2002; **60:**613–21.
9. Cohen S, Bano MC, Cima LG, Allcock HR, JVacanti JP , Vacanti CA and Langer R. Design of synthetic polymeric structures for cell transplantation and tissue engineering. *Clinical Materials* 1993; **13**:3-10.
10. Griffith LG. Emerging design principles in biomaterials and scaffolds for tissue engineering. *Ann N Y Acad Sci* 2002; **961**:83-95.

11. Bonassar LJ, Vacanti CA. Tissue engineering: the first decade and beyond. *J Cell Biochem Suppl* 1998; **30**:297-303.
12. Lysaght MJ, Hazlehurst AL. Tissue engineering: the end of the beginning. *Tissue Eng* 2004; **10**:309-320.
13. Griffith LG, Naughton G. Tissue Engineering. Current Challenges and Expanding Opportunities. *Science* 2002; **295**:1009-1014.
14. Vogel V, Baneyx G. The tissue engineeting puzzle: a molecular perspective. *Annu Rev Biomed Eng* 2003; **5**:441-463.
15. Vert M, Li MS, Spenlehauer G, Guerin P. Bioresorbability and biocompatibility of aliphatic polyesters. *J Mater Sci* 1992; **3**: 432-46.
16. Kim BS, Mooney DJ. Development of biocompatible synthetic extracellular matrices for tissue engineering. *Trends Biotechnol* 1998; **16**:224-230.
17. Freed LE, Vunjak-Novakovic G, Biron RJ, et al. Biodegradable polymer scaffolds for tissue engineering. *Nat Biotecl* 1994; **12**:689-693.
18. Salgado AJ, Coutinho OP, Reis RL. Bone tissue engineering: State of the art and future trends. *Macromol Biosci*.2004; **4**:743-765.
19. Dietmar W. Hutmacher. Scaffolds in tissue engineering bone and cartilage. *Biomaterials* 2000; **21**: 2529-2543.
20. Yu X, Bellamkonda RV. Tissue-engineered scaffolds are effective alternatives to autografts for bridging peripheral nerve gaps. *Tissue Eng* 2003, **9:**421-430.
21. Florian Groeber F, Monika Holeiter M, Martina Hampel M, Svenja Hinderer S and Layland KS. Skin tissue engineering — *In vivo* and *in vitro* applications. *Tissue Eng* 2011; **60**:352–366.

22. Ananta M, Brown RA, and Mudera V. A Rapid Fabricated Living Dermal Equivalent for Skin Tissue Engineering: An *In Vivo*Evaluation in an Acute Wound Model *Tissue Engineering Part A* 2012, **18**: 353-361.
23. Shevchenko RV, James SL and James SE. A review of tissue-engineered skin bioconstructs available for skin reconstruction. *J. R. Soc. Interface* 2010; **7**: 229-258.
24. Deitzel JM, Kleinmeyer J, Harris D, Tan NCB. The effect of processing variables on the morphology of electrospun nanofibers and textiles. *Polymer* 2001; **42**:261–72.
25. An Y, Tsang KKS, Zhang H: Potential of stem cell based therapy and tissue engineering in the regeneration of the central nervous system. *Biomed Mater* 2006; **1**:38-44.
26. Sundaray B, Subramanian V, Natarajan TS, Xiang RZ, Chang CC, Fann WS. Electrospinning of continuous aligned polymer fibers. *Appl Phys Lett* 2004; **84**:1222–4.
27. Skovronsky, D.M.; Lee, V.M.; Trojanowski, J.Q. Neurodegenerative diseases: New concepts of pathogenesis and their therapeutic implications. *Annu. Rev. Pathol* 2006; **1**: 151-170.
28. Girard C, Bemelmans A, Dufour N, Mallet J, Bachelin C, Nait-Oumesmar B, Evercooren AB, Lachapelle F. Grafts of brain-derived neurotrophic factor and neurotrophin 3-transduced primate schwann cells lead to functional recovery of the demyelinated mouse spinal cord. *J Neurosci* 2005; **25**:7924-7933.
29. Recknor JB, Recknor JC, Sakaguchi DS, Mallapragada SK. Oriented astroglial cell growth on micropatterned polystyrene substrates. *Biomaterials* 2004; **25:**2753-2767.
30. Song H, Stevens CF, Gage FH. Astroglia induce neurogenesis from adult neural stem cells. *Nature* 2002; **417:**39-44.
31. David RN, Andrew ER, Malcolm KH, John SF, David IF. Neurite infiltration and cellular response to electrospun polycaprolactone scaffolds implanted into the brain. *Biomaterials* 2009; **30:**4573-4580.

32. Keilhoff G, Stang F, Goihl A, Wolf G, Fansa H. Transdifferentiated mesenchymal stem cells as alternative therapy in supporting nerve regeneration and myelination. *Cell Mol Neurobiol* 2006; **26:**1233-1250.
33. Hadlock T, Sundback C, Hunter D, Cheney M and Vacanti J P. A polymer foam conduit seeded with Schwann cells promotes guided peripheral nerve regeneration. *Tissue Eng* 2000; **6:** 119–27.
34. Stokols S and Tuszynski M H. Freeze-dried agarose scaffolds with unaxial channels stimulate and guide linear axonal growth following spinal cord injury. *Biomaterials* 2006; **27:** 443–51.
35. Corey J M, Lin D Y, Mycek K B, Chen Q, Samuel S, Feldman E L and Martin D C. Aligned electrospun nanofibers specify the direction of dorsal root ganglia neurite growth. *J. Biomed. Mate. Res. A* 2007; **83:** 636–45.
36. Corey J.M, Gertz CC, Wang BS, Birrell LK, Johnson SL, Martin DC and Feldman EL. The design of electrospun PLLA nanofiber scaffolds compatible with serum-free growth of primary motor and sensory neurons. *Acta Biomater* 2008; **4**, 863-875.
37. Alluin O, Wittmann C, Marqueste T, Chabas JF, Garcia S and Lavaut MN. Functional recovery after peripheral nerve injury and implantation of a collagen guide. *Biomaterials* 2009; **30**:363–73.
38. Pfister LA, Papaloizos M, Merkle HP and Gander B. Nerve conduits and growth factor delivery in peripheral nerve repair. *J Peripher Nerv Syst* 2007; **12**:65–82.
39. Madduri S, Papaloizos M, and Gander B. Trophically and topographically functionalized silk fibroin nerve conduits for guided peripheral nerve regeneration. *Biomaterials* 2010; **31**: 2323–2334.

40. Yang, F. Eletcrospinning of nano/micro scale poly(L-lactic acid) aligned fibers and their potential in neural tissue engineering. *Biomaterials* 2005; **26**: 2603-2610.
41. Oh SH, Kim JH, Song KS, Jeon BH, Yoon JH, Seo TB, Namgung U, Lee IW and Lee JH. Peripheral nerve regeneration within an asymmetrically porous PLGA/Pluronic F127 nerve guide conduit**.** *Biomaterials* 2008; **29:**1601-1609.
42. Haile Y, Berski S, Drager G, Nobre A, Stummeyer K, Gerardy-Schahn R, Grothe C. The effect of modified polysialic acid based hydrogels on the adhesion and viability of primary neurons and glial cells. *Biomaterials* 2008; **29**:1880-1891.
43. Electrospun poly(3-caprolactone)/gelatin nanofibrous scaffolds for nerve tissue engineering Mobarakeh LG, Prabhakaran MP, Morshed, Esfahani MHN, Ramakrishna S .*Biomaterials* 2008; **29**: 4532–4539.
44. Gomez N and Schmidt CE. Nerve growth factor-immobilized polypyrrole: Bioactive electrically conducting polymer for enhanced neurite extension. *J Biomed Mater Res A*. 2007; **81**:1.
45. Schnell E, Klinkhammer K, Balzer S, Brook G, Klee D and Dalton P. Guidance of glial cell migration and axonal growth on electrospun nanofibers of polyepsilon- caprolactone and a collagen/poly-epsilon-caprolactone blend. *Biomaterials* 2007; **28**:3012–25.
46. Ciardelli G, Chiono V, Vozzi G, Pracella M, Ahluwalia A and Barbani N. Blends of poly(3-caprolactone) and polysaccharides in tissue engineering applications. *Biomacromolecules* 2005; **6**:1961–76.
47. Pfister LA, Alther E, Papaloizos M, Merkle HP and Gander B. Controlled nerve growth factor release from multi-ply alginate/chitosan-based nerve conduits. *Eur J Pharm Biopharm* 2008; **69**:563–72.

48. Formhals, A. Apparatus for producing artificial filaments from material such as cellulose acetate. US patent no. 1975504; 1934.
49. Shin YM, Hohman MM, Brenner MP, Rutledge GC. Electrospinning: a whipping fluid jet generates submicron polymer fibers. *Appl Phys Lett* 2001; **78**:1149–51.
50. Baumgarten PK. Electrostatic spinning of acrylic microfibers. *J Colloid Interface Sci* 1971; **36**:71–79.
51. Hayati AI and Bailey TF. Investigations into the mechanisms of electrohydrodynamic spraying of liquids. 1. Effect of electric-field and the environment on pendant drops and factors affecting the formation of stable jets and atomization. *J Colloid Interface Sci* 1987; **117**:205–221.
52. Berry JP. Electrostatically Produced Structures and Methods of Manufacturing. US Patent 4965110 (1990).
53. M. Cloupeau M, B. Prunet-Foch BP. Electrostatic spraying of liquids: Main functioning modes. *Tissue Eng*. 1990; **25**: 165-184.
54. Doshi J and Reneker DH. Electrospinning process and applications of electrospun fibers. *J Electrostat* 1995; **35**:151–60.
55. Ko FK. Nanofiber technology in nanotubes and nanofibers (advanced materials). Yury Gogotsi, editor. Taylor and Francis Group LLC 2006.
56. Fridrikh SV, Yu JH, Brenner MP, Rutledge GC. Controlling the fiber diameter during electrospinning. *Phys Rev Lett* 2003; **90**:1–4.
57. Wang H B, Mullins M E, Cregg J M, Hurtado A, Oudega M, Trombley M T and Gilbert R J. Creation of highly aligned electrospun poly-L-lactic acid fibers for nerve regeneration applications. *J. Neural. Eng* 2009; **6:** 016001.

58. Ajao JA, Abiona AA, Chigome S, Fasasi AY, Osinkolu GA and Maaza M. Electric-magnetic field-induced aligned electrospun poly (ethylene oxide) (PEO) nanofibers. *J Mater Sci* 2010; **45**:2324–2329.

59. Pokorny M and Velebny V. Collection method for extra aligned nanofibers deposited by Electrospinning. *Rev. Sci. Instrum* 2011; 82:055112

60. Yang F. Eletcrospinning of nano/micro scale poly(L-lactic acid) aligned fibers and their potential in neural tissue engineering. *Biomaterials* 2005, **26**, 2603-2610.

61. Chew S Y, Mi R, Hoke A and Leong K W. Aligned protein–polymer composite fibers enhance nerve regeneration: a potential tissue-engineering platform. *Adv. Funct. Mater.* 2007; **17:** 1288–96.

62. Yao L, O'Brien N, Windebank A and Pandit A. Orienting neurite growth in electrospun fibrous neural conduits. *J. Biomed. Mater. Res. B Appl. Biomater.* 2009; **90**: 483-491.

63. Gertz CC, Leach MK, Birrell LK, Martin DC, Feldman EL and Corey JM. Accelerated neuritogenesis and maturation of primary spinal motor neurons in response to nanofibers. *Dev. Neurobiol.* 2010; **70**: 589-603.